bioRxiv preprint doi: https://doi.org/10.1101/059477; this version posted June 17, 2016. The copyright holder for this preprint (which was not certified by peer review) is the author/funder, who has granted bioRxiv a license to display the preprint in perpetuity. It is made available under aCC-BY-NC-ND 4.0 International license.

DNA methylation plays a role on *in vitro* culture induced loss of virulence in *Botrytis cinerea*

Jimmy Breen[1], Luis Alejandro Jose Mur[2], Anushen Sivakumaran[2], Aderemi Akinyemi[2], Michael James Wilkinson[2], Carlos Marcelino Rodriguez Lopez[3*]

[1]Robinson Research Institute, University of Adelaide, North Terrace Campus, Adelaide SA 5005

[2]Institute of Biological, Environmental and Rural Sciences, Edward Llywd Building, Penglais Campus, Aberystwyth, Ceredigion, SY23 3FG, UK.

[3]Environmental Epigenetics and Genetics Group, School of Agriculture, Food and Wine, Waite Research Precinct, University of Adelaide, PMB 1, Glen Osmond, SA 5064, Australia.

Corresponding author

bioRxiv preprint doi: https://doi.org/10.1101/059477; this version posted June 17, 2016. The copyright holder for this preprint (which was not certified by peer review) is the author/funder, who has granted bioRxiv a license to display the preprint in perpetuity. It is made available under aCC-BY-NC-ND 4.0 International license.

Summary

- Little is known about the mechanisms causing loss of virulence in pathogenic fungi as a result of protracted culture. We studied the extent to which patterns of DNA methylation varied between virulent and reduced virulence derivative cultures of *Botrytis cinerea*, and identify the genes/genomic regions affected by these epigenetic modifications.
- *B. cinerea* was cultured *in vitro* for eight months involving subculture every four weeks. Fungal conidia were harvested at every four-week subculturing stage and inoculated onto *Arabidopsis thaliana* Col-0 plants for virulence testing. Global epi/genetic changes in *B. cinerea* during culture were assessed using methylation-sensitive amplified polymorphisms (MSAPs) on mycelium from eight different sub-culture time points and from mycelium recovered after eight months in culture and then inoculated onto *A. thaliana*. Culture induced epi/allele characterisation was carried out by whole genome sequencing and bisulfite sequencing of gDNA from samples after two and eight months in culture and after 8 months in culture and following inoculation onto an *A. thaliana* plant.
- Virulence declined with time in culture and recovered after one fungal generation on *A. thaliana*. MSAP data show that epi/genetic variation followed virulence changes during culture. Whole genome sequencing showed no significant genetic changes during culture. Conversely, bisulfite sequencing showed significant changes both on global and local methylation patterns.
- We suggest that virulence is a non-essential plastic character regulated by DNA methylation during protracted *in vitro* culture. We propose DNA methylation as a regulator of the high virulence/low virulence transition in *B. cinerea* and as a potential mechanism to control pathogenicity.

bioRxiv preprint doi: https://doi.org/10.1101/059477; this version posted June 17, 2016. The copyright holder for this preprint (which was not certified by peer review) is the author/funder, who has granted bioRxiv a license to display the preprint in perpetuity. It is made available under aCC-BY-NC-ND 4.0 International license.

Introduction

Botrytis cinerea is an ascomycete responsible for grey mould on hundreds of dicot plants that is able to feed on different plant tissues (1) and causes annually up to $100 billion in losses worldwide (2). The wide variety of symptoms on different organs and plant species may suggest that *B. cinerea* has a large 'arsenal of weapons' to attack its host plants. *B. cinerea* is well documented as a capable saprotroph and necrotroph with genetic types showing a trade-off between saprotrophic and necrotrophic capabilities (3). As other pathogens, *B. cinerea* undergoes transcriptional and developmental regulation to govern the outcome of pathogen/host interactions. Population dynamics between the two types have been linked to resource availability. Interestingly, chances in virulence levels have also been observed during protracted *in vitro* culture of *B. cinerea* (4). In fact, pathogenic fungi are notorious for losing virulence when successively subcultured *in vitro*. Degenerate cultures have been reported in a wide range of pathogenic fungi (5) but very little is known about why the cultures degenerate. Different factors have been described as possible effectors of the observed loss of virulence during culture including dsRNA mycoviruses (6,7), loss of conditional dispensable chromosomes (8,9) or culture induced selection of nonvirulent strains. However, one characteristic common to almost all *in vitro*-derived nonvirulent fungal strains is that their virulence is restored after one passage on their host (5). If attenuated strains recover virulence then loss of virulence cannot be explained by mycoviruses infection or chromosome loss. Furthermore, fungal strains in culture lose virulence irrespective of whether the parent culture was derived from a single spore or multi-spore colony (5), suggesting that there cannot be a culture induced selection of nonvirulent strains.

This observed reversible phenotype in response to changes in the environment could be associated to phenotypic plasticity (10). In 1942 C.H. Waddington (11) first proposed the

bioRxiv preprint doi: https://doi.org/10.1101/059477; this version posted June 17, 2016. The copyright holder for this preprint (which was not certified by peer review) is the author/funder, who has granted bioRxiv a license to display the preprint in perpetuity. It is made available under aCC-BY-NC-ND 4.0 International license.

term epigenotype to describe the interface between genotype and phenotype. Since then, a large body of research has been carried out to better understand the role of epigenetic regulatory systems in shaping the phenotype of higher organisms surviving in fluctuating environments (12,13). Epigenetic processes operate in a number of ways to alter the phenotype without altering the genetic code (14). These include DNA methylation, histone modifications, and mRNA editing and degradation by noncoding RNAs. Such processes are intimately entwined and often work in a synergistic way to ultimately achieve changes in phenotype (15). DNA methylation, and more specifically cytosine methylation (i.e. the incorporation of a methyl group to carbon 5 of the cytosine pyrimidine ring to form 5-methylcytosine (5-mC)) is probably the most studied epigenetic mechanism. It is present across many eukaryotic phyla, including plants, mammals, birds, fish, and invertebrates and provides an important source of epigenetic control for gene expression (16). In plants and animals, DNA methylation is known to be involved in diverse processes including transposon silencing, X-chromosome inactivation, and imprinting (17). In fungi, several studies have showed changes in overall 5-mC content during development in *Phymatotrichu omnivorum* (18) and *Magnaporthe oryzae* (19). Global patterns in DNA methylation has been previously shown to dramatically change in lichen fungi species when exposed to the algal symbiont (20). Methtylome sequencing in Ascomycetes has shown that this group of fungi present heavily methylated silent repeated loci and methylated active genes. Zemach et al, (21) reported a correlation between gene body methylation and *gene* expression levels in *Uncinocarpus reesii*. More recently, Jeon et al., (19) ascribed a developmental role for DNA methylation in *M. oryzae.* In this pivotal paper, it was demonstrated that gene DNA methylation density genes changes during development, and that transcript abundance is negatively affected by DNA methylation upstream and downstream of ORFs while gene body methylation has positive effects.

bioRxiv preprint doi: https://doi.org/10.1101/059477; this version posted June 17, 2016. The copyright holder for this preprint (which was not certified by peer review) is the author/funder, who has granted bioRxiv a license to display the preprint in perpetuity. It is made available under aCC-BY-NC-ND 4.0 International license.

Recent years have seen a dramatic increase in the depth of understanding of how epigenetic control mechanisms operate during plant/pathogen interactions (2,22). Conversely, little is known of the function of DNA methylation in relation to involvement of such processes in regulating traits related to virulence in fungal plant pathogens. Furthermore, no research has been done on the dynamic nature of DNA methylation during protracted culture and its possible contribution to loss of virulence. In this paper, our main objective is to examine if the observed loss of pathogenicity of *in vitro* cultures of *B. cinerea* can be related to differences in DNA methylation in their genomes. We used Methylation Sensitive Amplified Polymorphisms (MSAP) (23) as a preliminary approach in order to asses if the differences in pathogenicity observed during *in vitro* culture of *B. cinerea* could be correlated to changes in DNA methylation. For the high-throughput identification of Differentially Methylated Regions (DMRs) associated to the loss of pathogenicity in *B. cinerea* during *in vitro* culture we performed whole genome sequencing of sodium bisulfite modified DNA obtained from different times in culture. This approach provided us with the first confirmation that *B. cinerea* loss of pathogenicity induced by *in vitro* culture correlates with DNA methylation and targeted functional regions putatively involved in the epigenetic regulation of virulence in *B. cinerea*. We anticipate that these results will provide new targets for the control of *B. cinerea* caused disease. It also provides novel insights into the control of components that dictate saprotrophic and parasitic capability and proposes DNA methylation as a mechanism to control these processes.

Results

Pathogenicity analysis of *Botrytis cinerea*

bioRxiv preprint doi: https://doi.org/10.1101/059477; this version posted June 17, 2016. The copyright holder for this preprint (which was not certified by peer review) is the author/funder, who has granted bioRxiv a license to display the preprint in perpetuity. It is made available under aCC-BY-NC-ND 4.0 International license.

All isolates obtained from all culture time points produced lesions on *A. thaliana* to various extents (Figure 1A). As *B. cinerea* was successively cultured disease scores decreased over the eight month period (T0-T8) (Figure 1B). This loss of virulence with time in culture was significant from T3 onwards (T-Test $P < 0.05$) (Figure 1B). The disease scores for the T8P challenge did not differ significantly from those for those at T0 culture times suggesting recovered virulence following single passage through a plant (Figure 1B). Conversely, T8 virulence scores were significantly different from those obtained from T0 to T5 and T8P (T-Test $P < 0.05$) (Figure 1B). Fungal DNA content within the infected areas of the leaf was measured by quantitative PCR to confirm that *in planta* fungal development increased between T8 and T8P generation as described previously (24). Infected leaves with T0 and T8P cultures did not show significant differences in fungal DNA content (Figure 1C). However both showed significantly higher levels of fungal DNA (T-Test $P < 0.05$) when compared to those infected using T8 cultures (Figure 1C).

Analysis of genetic and epigenetic variance during culture using MSAPs

MSAP profiles generated a total of 74 loci (22 unique to *Hpa*II, 4 unique to *Msp*I and 48 common to both enzymes) for the 112 samples of eight *B. cinerea* culture times used in this study (T2-T8P). Multivariate analysis of the MSAP profiles revealed that epigenetically, *B. cinerea* became progressively more dissimilar to the first time point analyzed (T2) with culture age (Figure 2). Both, PCoA (Figure 2A and C) and estimated PhiPT values (Figure 2B) showed higher levels of time in culture induced variability when using *Hpa*II than when using *Msp*I. PCoA shows that samples cultivated for 3, 4, 5, 6, and 7 months occupied intermediate Eigenspace between samples cultivated for 2 and 8 months (Figure 2C). Furthermore, a partial recovery of the epigenetic profile was observed on samples cultured for 8 months after one fungal generation on the host plant (T8P) (Figure 2C). Calculated

bioRxiv preprint doi: https://doi.org/10.1101/059477; this version posted June 17, 2016. The copyright holder for this preprint (which was not certified by peer review) is the author/funder, who has granted bioRxiv a license to display the preprint in perpetuity. It is made available under aCC-BY-NC-ND 4.0 International license.

PhiPT values between each time point and T2 samples show an increase in epigenetic distance with time in culture when samples were restricted with both enzymes. AMOVA analysis shows that the calculated PhiPT values were significantly different ($P<0.05$) between T2 and time points T6, T7, T8 and T8P when using *Msp*I and T7, T8 and T8P when using *Hpa*II (Figure 2B).

B. cinerea **genome resequencing**

To determine if any of the *in vitro* culture variability detected using MSAP analysis could be attributed to genetic changes DNA extractions from 3 independent cultures from two time points (1 month (T1) and 8 months (T8) in culture) were pooled, sequenced and compared to the *B. cinerea* B05.10 genome sequence. Both samples were sequenced to an average depth of 37.47x (35.64x for the 1-month culture and 39.30x for the 8-month culture) with an average of 80% of reference bases being sequenced to a depth greater than 10x. After filtering for coverage greater than 10x and >30 variant quality 186,275 variants from the *B. cinerea* B05.10 reference genome were identified between both samples, with 174,456 variants being shared between both time points (i.e. T1 = T8). Additional filtering was used to remove multi-allelic variants, variants with missing data in one sample and variants with an observed allele frequency less than 0.5 (25). This filtering reduced the number of non-shared variants to 2,331, of which 1,030 (44%) were small insertions and deletions (INDELs) and 1,301 (56%) SNPs. CooVar (Vergara et al. 2012) was used to determine whether the detected variants altered specific annotations (genes, promoters etc). Of the 2,331 variants analysed, 454 were within genes including: 251 synonymous variants, 198 non-synonymous mutations (193 causing mis-sense variations and 5 causing premature stop codons (non-sense mutations) all located in the genes with unknown functions (BC1G_07064, BC1G_08869,

bioRxiv preprint doi: https://doi.org/10.1101/059477; this version posted June 17, 2016. The copyright holder for this preprint (which was not certified by peer review) is the author/funder, who has granted bioRxiv a license to display the preprint in perpetuity. It is made available under aCC-BY-NC-ND 4.0 International license.

BC1G_08189, BC1G_12710 and BC1G_01150). An additional 5 variants that altered predicted splice junctions were also identified.

We next focused the search for variants within the sequence of 1577 *B. cinerea* genes with known function including: secondary metabolism (i.e. sesquiterpenecyclases, diterpenecyclases, paxillin-like enzymes, fusiccocin-like enzymes, Phytoene synthases, non-ribosomal peptide synthetases, polyketides synthases, chalcone synthases, DiMethylAllyl Tryptophan Synthases) (26), conidiation (26), sclerotium formation (25), mating and fruit body development (26), apoptosis (26), housekeeping (26), signalling pathways (G protein-coupled receptors, MAP kinases, heterotrimeric G proteins, cAMP signalling components and Ca^{2+} -related signalling) (26) and virulence *senso lato* genes (147 genes were duplicated, i.e., present in more than one category). The virulence *sensu lato* genes included: 12 appressorium-associated genes (26), 17 virulence *sensu stricto* genes (27) and 1155 plant cell wall disassembly genes (CAZyme genes) (28). Of the 1577 tested genes, 68 (4.3%) contained one or more variants between T1 and T8 (See Table 1 and Supplementary Table 1 for a comprehensive list of genes with variants).

***B. cinerea* whole-genome bisulfite sequencing**

To validate and characterise the observed DNA methylation changes during culture of *B. cinerea* using MSAP analysis, we generated genome-wide DNA methylation maps across the fungal genome by conducting whole genome bisulphite sequencing (BS-seq) from triplicated genomic DNA extractions from mycelia of two different culture ages (1 month (T1) and 8 months (T8)) and from samples culture for eight months and then inoculated onto an *A. thaliana* plant (T8P). BS-seq of these samples yielded 187.5 million reads ranging from 12.61 to 34.05Gbp per sample after quality filtering. Mapping efficiency of each replicate ranged

bioRxiv preprint doi: https://doi.org/10.1101/059477; this version posted June 17, 2016. The copyright holder for this preprint (which was not certified by peer review) is the author/funder, who has granted bioRxiv a license to display the preprint in perpetuity. It is made available under aCC-BY-NC-ND 4.0 International license.

from 54.3 to 67.6%, resulting in samples that generated between 33 and 55x coverage of the 42.66Mbp genome (Supplementary Table 2). This is the highest genome coverage for bisulfite sequencing on any fungi to date. Each sample, covered over 91-93% of all cytosines present in the genome (Table 2), with all samples having at least 81% of cytosines covered by at least four sequencing reads, allowing methylation level of individual sites to be determined with reasonable confidence.

Bisulfite sequencing identified an average of 15716603 mC per sample, indicating an average methylation level of 0.6% with varying levels in each sample (Supplementary Table 2). The most common methylated context was CHH followed by CG and CHG (where H is A, C or T) (Supplementary Table 2). Although global levels of mC did not significantly change with culture time, methylation on contexts CG and CHG increased significantly (T-test, p=0.0008 and 0.0018) between 1 (T1) and 8 (T8) months in culture (Figure 3A). Both types of methylation showed a decreasing trend (not significant) on samples recovered from eight month old cultures inoculated onto *A. thaliana* (T8P) (Figure 3A). Conversely, methylation on all C and CHH showed a non-significant increasing trend with age culture (T1<T8<T8P). Analysis of local levels of DNA methylation across the largest *B. cinerea* contig (Supercontig 1.1) showed that DNA methylation is not evenly distributed but clustered in certain regions (Figure 3B-D). Observed clustering patterns were similar in all analysed samples (Figure 3B-D).

In order to investigate the influence of the different genomic features on DNA methylation we determined the distribution and density of mCs on 82 randomly selected genes (Supplementary Table 3) (exons and introns), and promoters (defined here as 1.5 kb upstream

bioRxiv preprint doi: https://doi.org/10.1101/059477; this version posted June 17, 2016. The copyright holder for this preprint (which was not certified by peer review) is the author/funder, who has granted bioRxiv a license to display the preprint in perpetuity. It is made available under aCC-BY-NC-ND 4.0 International license.

of the Transcription Starting Site (TSS)). This analysis showed that on the randomly selected genes mC proportion peaks 250bp upstream of TSS and decreases sharply before of the start of the coding sequences (Figure 4). When the different time points were compared at this site, mC showed an increase (T1<T8<T8P) in parallel with that observed at a whole genome level (Figure 3A).

The same methylation density analysis was then carried out for five loci corresponding to four housekeeping genes in Botrytis (i.e., G3PDH (Glyceraldehyde 3-phosphate dehydrogenase) (BC1G_09523.1); HSP60 (Heat Shock Protein 60) (BC1G_09341.1); Actin (BC1G_08198.1 and BC1G_01381.1) and Beta Tubulin (BC1G_00122.1). All five Loci present low levels of DNA methylation in every context and no changes in DNA methylation were observed between time points (i.e., T1, T8 and T8P) (Data not shown).

Finally, methylation density was analysed on 131 genes encoding putative CAZymes secreted by *B. cinerea* upon plant infection (Supplementary Table 3) (28). As a whole, these genes showed the same methylation pattern as described above for the 82 randomly selected genes with an increase in methylation upstream of the TSS (Figure 5A). More interestingly, these genes showed higher levels of methylation after 8 months in culture than at T1 and aT8P. This observed increase in global methylation on T8 samples seems to be due to an increase on the CHG and CG (Figure 5B-C) contexts. Conversely, CHH (Figure 5D) showed higher levels of methylation on the T8P samples, following the general trend observed both at a whole genome level (Figure 3A) and by the randomly selected genes (Figure 4).

Detection of culture induced DMRs

bioRxiv preprint doi: https://doi.org/10.1101/059477; this version posted June 17, 2016. The copyright holder for this preprint (which was not certified by peer review) is the author/funder, who has granted bioRxiv a license to display the preprint in perpetuity. It is made available under aCC-BY-NC-ND 4.0 International license.

In order to identify the loci presenting significant DMRs between culture times (T1, T8 and T8P) we compared the methylation levels across the whole genome of all samples using a sliding window analysis conducted using swDMR software (https://code.google.com/p/swdmr/). The significance of the observed DMRs was determined using a three sample Kruskal-Wallis test. Analysis of DMR length distribution showed DMRs sizes ranging from 12 to 4994bp (Figure 6A). This approach identified 2822 regions significantly differentially methylated in one of the samples compared to the other two for all mCs (Table 2, Supplementary Table 4). The analysis of the methylation levels on DMRs suggests these suffer a decrease in methylation in all contexts (CG, CHG and CHH) during time in culture (from T1 to T8) followed by a recovery of DNA methylation levels after culture on *A. thaliana* (T8P) (Figure 6b). However, T8 showed a larger number of outlier DMRs showing levels of methylation significantly higher than the average (Figure 6B). When studied individually, changes in methylation within DMRs between samples presented two main pattern types (Table 2, Supplementary Table 4): **1.** 57.3% of the detected DMRs showed a recovery pattern after samples culturing in *A. thaliana*. (i.e., Level of methylation was not significantly different between T1 and T8P samples but they were higher or lower than T8 (T1=T8P<> T8 (FDR< 0.01))). **2.** The rest of the DMRs showed a non-recovery pattern (i.e., T1<> T8P (FDR< 0.01)). Two subtypes where found for DMRs showing a DNA methylation recovery pattern: **1.** DMRs showing an increase in methylation with time in culture (T1=T8P <T8 (26.82%) (defined as Type 0 hereafter) and **2.** DMRs showing a decrease in methylation level with time in culture (T1=T8P > T8 (30.47%)) (Type 2). Equally, non-recovery DMRs can be divided into two categories: **1.** DMRs showing a decrease in methylation level with time in culture and no change in methylation level when culture on *A. thaliana* (T0>T7=T7P (16.02%)) (Type 1a) and **2.** DMRs not showing changes in methylation level during culture but an increase in methylation level when cultured on *A.*

bioRxiv preprint doi: https://doi.org/10.1101/059477; this version posted June 17, 2016. The copyright holder for this preprint (which was not certified by peer review) is the author/funder, who has granted bioRxiv a license to display the preprint in perpetuity. It is made available under aCC-BY-NC-ND 4.0 International license.

thaliana (T0=T7<T7P (26.68%)) (Type 1b). Interestingly the expected pattern where DMRs showed an increase in methylation level with time in culture and no change in methylation level when cultured on *A. thaliana* (T1<T8=T8P) was not observed.

2384 (84.5%) of the total detected DMRs for all mCs overlapped with 3055 *B. cinerea* (Table 3) while 438 (15.5%) mapped to intergenic regions. Of the 3055 genic regions overlapping with DMRs, 1709 (56%) were promoters (considered here 1.5kb before TSS) and 2994 (98%) were body of genes (with 1648 (53.9%) genes overlapping with a DMR both on the promoter and the gene body) (Table 3, Supplementary Table 5). The same analyses were carried out to detect DMRs for CG, CHG and CHH (where H is A, C or T) contexts. This generated 70, 82 and 1248 DMRs respectively for each context (Table 3, Supplementary Table 4). Of these, 91.4% (CG), 89.0% (CHG) and 85.2% (CHH) overlapped with 68, 84 and 1339 genes respectively (Table 4, Supplementary Table 5).

Finally, we conducted a search for DMRs overlapping with 1577 *B. cinerea* genes with known function including: secondary metabolism (i.e. sesquiterpenecyclases, diterpenecyclases, paxillin-like enzymes, fusiccocin-like enzymes, Phytoene synthases, non-ribosomal peptide synthetases, polyketides synthases, chalcone synthases, DiMethylAllyl Tryptophan Synthases) (26), conidiation (26), sclerotium formation (25), mating and fruit body development (26), apoptosis (26), housekeeping (26), signalling pathways genes (G protein-coupled receptors, MAP kinases, heterotrimeric G proteins, cAMP signalling components and Ca^{2+}-related signalling) (26) and virulence *senso lato* genes (147 genes were duplicated, i.e., present in more than one category). The virulence *sensu lato* genes included: 12 appressorium-associated genes (26), 17 virulence *sensu stricto* genes (27)

bioRxiv preprint doi: https://doi.org/10.1101/059477; this version posted June 17, 2016. The copyright holder for this preprint (which was not certified by peer review) is the author/funder, who has granted bioRxiv a license to display the preprint in perpetuity. It is made available under aCC-BY-NC-ND 4.0 International license.

and 1155 plant cell wall disassembly genes (CAZyme genes) (28). Of these, 478 genes (30.3%) overlapped with one or more detected DMRs (See Table 1 and Supplementary Table 6 for a comprehensive list of genes overlapping with DMRs).

Discussion

Previous studies have shown that protracted *in vitro* culture of pathogenic fungi reduces virulence (6–9) and that virulence levels recover after a single passage on their host in a significant number of species (5). This loss/recovery of virulence cycle suggests a plastic regulation of the trait. However, very little is known about why virulence degenerates in culture or what are the molecular mechanisms regulating these changes. In this study, we present, to our knowledge, the first proof that global and local changes in DNA methylation are linked to virulence changes during *in vitro* culture. Furthermore, here we present the first DNA methylome for the plant pathogen *B. cinerea*.

As expected, we found that virulence of *B. cinerea* cultures significantly decreases with culture age, and that virulence levels recover after one passage on *A. thaliana*. More surprisingly, analysis of global methylation pattern changes using MSAP profiles showed an increasing deviation from the original profiles with time in culture. This observed accumulation of somaclonal variation as culture progressed showed a positive linear correlation with the observed changes in virulence (R^2=0.5, P=0.002 and R^2=0.5 P=0.007, for epigenetic distances calculated using *Hpa*II and *Msp*I respectively). Such correlation between time in culture and genetic/epigenetic somaclonal variation is consistent with accumulation of sequence and/or DNA methylation changes with time in culture as previously reported for other species when cultivated *in vitro* (15,29). Moreover, these results are consistent with

bioRxiv preprint doi: https://doi.org/10.1101/059477; this version posted June 17, 2016. The copyright holder for this preprint (which was not certified by peer review) is the author/funder, who has granted bioRxiv a license to display the preprint in perpetuity. It is made available under aCC-BY-NC-ND 4.0 International license.

previous reports of high levels of somaclonal variability appearing during *in vitro* culture of phytopathogenic fungi, which affect the level of virulence of the culture isolates (30). However, the detected genetic/epigenetic distance after eight months in culture (T8) significantly decreased after a single passage of the cultured fungus on *A. thaliana* (T8P) suggesting a plastic change in virulence that cannot be explained only by genetic causes.

Whole genome resequencing of six DNA samples taken at two time points (one month and eight month) yielded a total of 2,331 variants of which 454 were within genes. Interestingly, only these included 198 non-synonymous mutations (193 causing missense variations and five causing premature stop codons (non-sense mutations). We then examined the appearance of genetic variants in 1577 *B. cinerea* genes with known function of which only 4.3% showed variants. Moreover just eight genes (0.5% of the total) presented variants that were not silent mutations, or led to a conservative missense codon or a synonymous codon. Of the 1184 genes associated to virulence included in the analysis, a similar proportion (0.5%) presented a variant that could affect the virulence phenotype. All of these genes were plant cell wall disassembly genes (CAZyme genes (31)). This low level of detected genetic variants and specially the lack of variants on virulence *sensu stricto* genes induced by protracted *in vitro* culture suggests that genetic variation might not be the only cause of virulence loss during in vitro culture of *B. cinerea* as shown previously for other species (25).

This suggests that changes in DNA methylation at a genome level could be associated to the observed loss of virulence during in vitro culture. To validate this hypothesis we carried out the sequencing of the methylomes of nine samples from three culture time points (T1, T8 and T8P). In average all genomes presented low levels of DNA methylation (0.6%) as reported

bioRxiv preprint doi: https://doi.org/10.1101/059477; this version posted June 17, 2016. The copyright holder for this preprint (which was not certified by peer review) is the author/funder, who has granted bioRxiv a license to display the preprint in perpetuity. It is made available under aCC-BY-NC-ND 4.0 International license.

for other fungal species (21). DNA methylation was not evenly distributed across contigs but clustered in certain regions following a mosaic pattern (32) with higher levels of methylation in regions with lower abundance of genes. Such clustering patterns have been previously observed in pathogenic fungi linked to transposable elements rich and gene poor regions (19) and have been shown to be dynamic following fungal development (19). Interestingly, the observed clustering patterns were similar in all analysed culture time points suggesting that the methylation changes detected here are not associated to progression in development occurred during culture. However, global methylation levels varied with sequence context (with CHH > CG > CHG) and time in culture. In brief, global methylation levels on CGs and CHGs increased significantly between 1 (T1) and 8 (T8) months in culture. In both cases, methylation showed a decreasing trend (not significant) on samples recovered from 8 months old cultures inoculated onto *A. thaliana* (T8P). This observed change in methylation levels supports MSAP results that showed an increase of epigenetic variation with time in culture that was only partially recovered n T8P cultures.

Previous genome wide studies have shown that gene methylation in the monophyletic Ascomycota phylum varies greatly. For example, in *Neurospora crassa* DNA methylation is not found in gene bodies. However gene body methylation has been reported in other species such as, *Candida albicans*, *Uncinocarpus reesii* and *Magnaporthe oryza* (16,19,21) while promoter methylation has only been reported in *M. oryza* (19). Analysis of the effect of methylation distribution and density on gene expression has shown that gene body methylation has positive effects on gene expression (19,21) while promoter methylation has a negative effect (19). Our analysis of methylation distribution in *B. cinerea genes* showed an increase in methylation approximately 800bp upstream of the TSS followed by a sharp decrease at the TSS as shown by Jeon et al (2015) in *M. oryza* mycelia. More interestingly,

bioRxiv preprint doi: https://doi.org/10.1101/059477; this version posted June 17, 2016. The copyright holder for this preprint (which was not certified by peer review) is the author/funder, who has granted bioRxiv a license to display the preprint in perpetuity. It is made available under aCC-BY-NC-ND 4.0 International license.

CAZyme genes showed a second increase in methylation density after the TSS indicating that at least some *B. cinerea* genes present gene body methylation.

Comparative analysis between culture time points showed that while house-keeping genes did not show changes in DNA methylation density between culture time points, both the randomly selected and the CAZyme genes showed an increase in promoter methylation with time in culture similar to that observed at a whole genome scale (i.e. T1<T8). However, CAZyme genes showed a recovery (not observed on the randomly selected genes) of the original methylation levels after a single passage on *A. thaliana* (i.e. T1=T8P<T8). Conversely, global methylation levels on the CAZyme gene bodies showed a positive correlation with virulence levels (T1=T8P>T8). This observed increase in promoter methylation on T8 samples seems to be due to an increase on the CHG and CG contexts, while higher gene body methylation on T1 and T8P samples seem to be due to changes on the CHH context. CAZyme genes encode proteins that breakdown, biosynthesise and modify plant cell wall components and are highly expressed during plant invasion in *B. cinerea* (28,31). This gene family, should therefore, be readily accessible to the transcriptional machinery in the virulent form of pathogenic fungi. Interestingly, our results show a correlation between virulence levels in T1, T8 and T8P samples and methylation features in CAZyme genes that have positive effects on gene expression, i.e. high gene body methylation (19,21) and low promoter methylation (19) in high virulence cultures (T1 and T8P) and the opposite in the low virulence culture (T8).

To determine the significance of the observed changes in DNA methylation between culture time points we performed an analysis of regional differential methylation identifying 2822

bioRxiv preprint doi: https://doi.org/10.1101/059477; this version posted June 17, 2016. The copyright holder for this preprint (which was not certified by peer review) is the author/funder, who has granted bioRxiv a license to display the preprint in perpetuity. It is made available under aCC-BY-NC-ND 4.0 International license.

significant DMRs in one time point compared to the other two for all mCs. Globally, DMRs show a decrease in methylation between T1 to T8 in all contexts (CG, CHG and CHH) followed by a recovery of DNA methylation levels after culture on *A. thaliana* (T8P). This seem to contradict the observed changes in global DNA methylation levels which showed an increasing trend (T1<T8<T8P). However, T8 showed a larger number of outlier DMRs showing levels of methylation significantly higher than the average suggesting that not all predicted DMRs followed the same pattern of demethylation followed by remethylation. Furthermore, similar differences between global and local DNA methylation levels have been reported previously in different organisms (19,33). More importantly, 68.3% of the culture induced DNA methylation changes (i.e. Type 0, 2 and 1a, which accounts for 57.3% of the total detected DMRs) showed a recovery pattern after samples culturing in *A. thaliana*. Suggesting that a majority of the epigenetic changes accumulated during *in vitro* culture are reset to their original state after a single passage on the host. Interestingly, 26.7% of the observed changes (Type 1b) were not induced *in vitro* culture but by the host. This highlights, as shown before in other pathogens (2,34,35), the importance of epigenetic mechanisms in host/pathogen interactions.

Of the total detected DMRs for all mCs 84.5% overlapped with one or more genes suggesting that the great majority of *in vitro* culture induced DNA methylation changes happen on genic regions. This overlap of individual DMRs with one than more gene is probably partially due to the small average size of intergenic regions (778 to 958bp) and genes (744 to 804 bp) in *B. cinerea* (26). Analysis of DMRs overlapping with 1577 genes with known function revealed that 30.3% of the total overlapped with DMRs. Ten gene functional groups (house-keeping, apoptosis, conidiation, mating and fruit body development, secondary metabolism, signaling, sclerotium formation, appresorium formation, virulence and CAZYme genes). House-

bioRxiv preprint doi: https://doi.org/10.1101/059477; this version posted June 17, 2016. The copyright holder for this preprint (which was not certified by peer review) is the author/funder, who has granted bioRxiv a license to display the preprint in perpetuity. It is made available under aCC-BY-NC-ND 4.0 International license.

keeping genes did not overlap with any DMRs while genes associated to apoptosis and conidiation showed the higher percentage of overlapping with DMRs (40.0 And 37.5% respectively). Remarkably, both biological processes have been previously shown to be affected by DNA methylation (19,36,37). Interestingly, the 98% of these DMRs overlapped, at least partially, with gene bodies while 2.4% and 15.6% overlapped only with promoters or gene bodies respectively. Taken collectively, this indicates that *B. cinerea* genes in general and gene bodies in particular are epigenetically plastic genomic regions in *B. cinerea.* More remarkably, when DMRs were defined using each DNA methylation context independently (i.e. CG, CHG and CHH), the large majority (89.1% of all DMRs and 89.9% of those overlapping with genes) were linked to changes on the CHH context, which suggests that DMRs in this context are the reason for the observed changes in detected CAZyme gene body methylation associated to higher levels of virulence.

Interestingly, similar regional changes in DNA methylation have been previously associated to the developmental potency of fungal cells (19). In their work, Jeon et al (2015) showed how fungal totipotent cells (mycelia) present higher global methylation levels while cells determined to host penetration (appresoria) present a higher number of genes with methylated cytosines but lower global levels of DNA methylation. Changes of global levels of DNA methylation have also been previously reported between the free-living and symbiotic forms of the plant ectomycorhrizal (EcM) fungus *Tuber melanosporum* (38) and in the Cladonia lichen fungus (20). In both cases, the genomes of the culture free mycelia presented lower levels of DNA methylation when compared to the genomes of the fungal tissues associated to the plant (38) or the algae (20) respectively. Conversely, our results suggest that protracted culture of *B. cinerea* induces a hypermethylated, low pathogenic free-living form adapted to the absence of the host or the abundance of nutrients in the culture media. Remarkably,

bioRxiv preprint doi: https://doi.org/10.1101/059477; this version posted June 17, 2016. The copyright holder for this preprint (which was not certified by peer review) is the author/funder, who has granted bioRxiv a license to display the preprint in perpetuity. It is made available under aCC-BY-NC-ND 4.0 International license.

dynamic DNA methylation has been proposed as regulator of phenotypic plasticity in response to nutrient availability and interaction with the host (39).

Although the presence of both hypermethylation and hypomethylation on the free living forms of pathogenic and symbiotic fungi could be intuitively contradictory, our results could better understood if fungal lifestyles (saprotrophism, symbiosis and pathogenesis) are considered as part of a continuum (40). In this model we propose that global DNA methylation levels are inversely correlated to environmental challenge. Low environmental challenge induces high levels of methylation that in turn reduce the expression of genes. On the contrary, DNA methylation decreases as environmental challenge increases allowing the expression of genes needed to confront such challenge (Figure 7). In fact, genome expansion by proliferation of transposable elements (TEs), which induces genome hypermethylation (19), has been associated to the evolution of obligated pathogenic fungi from saprotrophic species (40). Moreover, hypomethylation of TEs found within 1 kb of a gene has been associated to increased gene expression in TE rich plant-symbiotic fungi (38). It is tempting to speculate that the observed change in global and local levels of DNA methylation during *in vitro* culture could be part of a mechanism that confers plasticity to the *B. cinerea* genome to adapt to different environments (i.e. high/low levels of available nutrients or presence/absence of a host). Butt et al (2006) proposed that *in vitro* culture induced loss of virulence could be the reflexion of an adaptive trait selected to promote energy efficiency i.e. by turning off virulence genes in the absence of the host or in environments rich in freely available nutrients. The authors also proposed that this trait could become maladaptive since it restricts the pathogen to a saprophytic mode (5). Environmentally induced epigenetic adaptive changes have been predicted to have the potential to induce evolutionary traps leading to maladaptation (41,42). However, in this case the complete reversibility of the

bioRxiv preprint doi: https://doi.org/10.1101/059477; this version posted June 17, 2016. The copyright holder for this preprint (which was not certified by peer review) is the author/funder, who has granted bioRxiv a license to display the preprint in perpetuity. It is made available under aCC-BY-NC-ND 4.0 International license.

reduced virulence phenotype induced by protracted culture suggests that this might not be the case.

In our view, the availability of an increasingly large number of sequenced genomes and methylomes from pathogenic fungi together with our ability to decipher the associations between changes in DNA methylation and virulence will stimulate our understanding of the mechanisms involved in the control of pathogenicity on these species. Moreover, the analysis of DMRs could potentially be used to predict gene function in non-model fungal species or even to predict pathogenicity in wild strains. More importantly, if the epigenetic regulation of the transition between the pathogenic and the saprotrophic states that we propose here applies broadly to other pathogenic fungi, our findings will open the door to a new type of non-lethal fungicide aimed at maintaining pathogenic fungi as saprotrophic that by its nature would reduce the appearance of resistant strains.

Materials and Methods

Botrytis cinerea culture and inoculation

7 *Botrytis cinerea* cultures (IMI169558 isolate (43)) were initiated from a single frozen inoculum and cultured and harvested for 32 weeks as stated in Johnson et al (44). After 4 weeks in culture (T0) the initial culture was subcultured to 7 plates containing fresh medium. Mycelium from each plate was subsequently subcultured every 4 weeks (1 month hereafter) to fresh medium. A mycelium sample was taken for DNA extraction from all replicates and conidia harvested for virulence analysis (44) from five replicates at every subculture. For assessments of infection phenotypes, single leaves from five *Arabidopsis thaliana* Col 0 plants (leaf stage 7 or 8 as defined by (45)) were inoculated with 5 µl of spore suspension

bioRxiv preprint doi: https://doi.org/10.1101/059477; this version posted June 17, 2016. The copyright holder for this preprint (which was not certified by peer review) is the author/funder, who has granted bioRxiv a license to display the preprint in perpetuity. It is made available under aCC-BY-NC-ND 4.0 International license.

collected at each subculture time (T0-T8), pipetted onto the adaxial surface of the leaf. Controls were inoculated with PDB. Finally, after the T8 challenge, *B. cinerea* was isolated from the infected areas, cultured and immediately used to challenge *A. thaliana* plants to test virulence recovery (Figure S1) (T8P). Plants remained under Stewart Micropropagators to sustain a relative humidity of 50–80% and lightly watered every 24 h.

Plant material

A. thaliana Col-0 seeds were obtained from the Nottingham Arabidopsis Stock Centre (NASC). Plants were cultivated as stated in (46) in Levington Universal compost in trays with 24-compartment inserts. Plants were maintained in Conviron (Controlled Environments Ltd) growth rooms at 24 C with a light intensity of 110 µmol m-2 s-2 and an 8 h photoperiod for 4 weeks. For ease of treatment, plants were transferred to Polysec growth rooms (Polysec Cold Rooms Ltd, UK; http://www.polysec.co.uk/), maintained at the same conditions.

DNA isolation

126 *B. cinerea* genomic DNA (gDNA) extractions were performed (from 2 replicates of each of the 7 plates at *in vitro* time point (T1-T8) and from of the last time point culture transplanted onto to *A. thaliana* (T8P)) using the DNeasy 96 Plant Kit (Qiagen, Valencia, CA) and the Mixer Mill MM 300 (Retsch, Germany). Isolated DNA was diluted in nanopure water to produce working stocks of 10 ng.µl^{-1}. DNA from *B. cinerea* inoculated *A. thaliana* was extracted from five leaf samples at each time point of using a DNeasy Mini Kit (Qiagen, Valencia, CA) and the Mixer Mill MM 300 (Retsch, Germany). DNA samples were diluted to 1 ng.µl^{-1} nanopure water.

bioRxiv preprint doi: https://doi.org/10.1101/059477; this version posted June 17, 2016. The copyright holder for this preprint (which was not certified by peer review) is the author/funder, who has granted bioRxiv a license to display the preprint in perpetuity. It is made available under aCC-BY-NC-ND 4.0 International license.

Scoring *B. cinerea* lesion phenotypes

Disease lesions were assessed 3 days post inoculation. A weighted scoring method was used to categorize *B. cinerea* lesion phenotypes (47). High virulence symptoms (water-soaking, chlorosis, and spreading necrosis) were conferred a range of positive scores and the resistant symptoms (necrosis limited to inoculation site) were given negative scores (Figure 1A). A weighted score was produced arithmetically from the lesion scores of replicates. Inoculated *A. thaliana* leaves at T0, T8 and T8P were collected 3 days after inoculation for estimation of *in planta* fungal development by quantitative PCR **(Figure S1)**.

Estimation of *in planta* fungal development by quantitative PCR

Quantitative real-time PCR (qPCR) reactions (25 µl) were prepared by mixing 10 µl DNA solution with 12.5 µl of SYBR™ Green Mastermix (Applied Biosystems, UK) and primers (to a final concentration of 300 nM). Primer for Arabidopsis to generated a 131 bp amplicon of the Shaggy-kinase-like gene (ASK) ((iASK1: CTTATCGGATTTCTCTATGTTTGGC; iASK2: GAGCTCCTGTTTATTTAACTTGTACATACC). Primers for *B. cinerea.* (CG11: AGCCTTATGTCCCTTCCCTTG; CG12: GAAGAGAAATGGAAAATGGTGAG to generated a Cutinase A gene 58 bp amplicon (24). qPCRs were carried out using a Bio-Rad ABI7300 thermocycler amplifying using the following conditions: 15 min at 95 °C followed by 50 cycles of 95 °C for 15 s, 58 °C for 30 s and 72 °C for 1 min. This was followed by a dissociation (melting curve), according to the software procedure. Serial dilutions of pure genomic DNA from each species were used to trace a calibration curve, which was used to quantify plant and fungal DNA in each sample. Results were expressed as the CG11/iASK ratio of mock-inoculated samples.

bioRxiv preprint doi: https://doi.org/10.1101/059477; this version posted June 17, 2016. The copyright holder for this preprint (which was not certified by peer review) is the author/funder, who has granted bioRxiv a license to display the preprint in perpetuity. It is made available under aCC-BY-NC-ND 4.0 International license.

MSAP procedure

We used a modification of the MSAP methods (48,49) to reveal global variability in CG methylation patterns between *B. cinerea* samples. A total of 14 samples per time point (T1 to T7P) were analysed (2 replicated DNA extractions per culture plate). For each individual sample, 50ng of DNA were digested and ligated for 2 h at 37°C using 5U of *Eco*RI and 1U of *Msp*I or *Hpa*II (New England Biolabs), 0.45 µM *Eco*RI adaptor, 4.5 µM *Hpa*II adaptor (Supplementary Table 7 for oligonucleotide sequences) and 1U of T4 DNA ligase (Sigma) in 11 µl total volume of 1X T4 DNA ligase buffer (Sigma), 1µl of 0.5M NaCl, supplemented with 0.5 µl at 1mg/ml of BSA. Enzymes were then inactivated by heating to 75°C for 15 min. Following restriction and adaptor ligation there followed two successive rounds of PCR amplification. For preselective amplification, 0.3 µl of the restriction/ligation products described above were incubated in 12.5 µl volumes containing 1X Biomix (Bioline, London, UK) with 0.05 µl of Preamp EcoRI primer and 0.25 µl Preamp HpaII/MspI (both primers at 10 uM) (Supplementary Table 7) supplemented with 0.1 µl at 1mg/ml of BSA. PCR conditions were 2 min at 72_C followed by 30 cycles of 94_C for 30 s, 56_C for 30 s and 72_C for 2 min with a final extension step of 10 min at 72°C. Selective PCR reactions were performed using 0.3 µl of preselective PCR reaction product and the same reagents as the preselective reactions but using FAM labelled selective primers (E2/H1; Supplementary Table 7). Cycling conditions for selective PCR were as follows: 94°C for 2 min, 13 cycles of 94°C for 30 s, 65°C (decreasing by 0.7°C each cycle) for 30 s, and 72°C for 2 min, followed by 24 cycles of 94°C for 30 s, 56°C for 30 s, and 72°C for 2min, ending with 72°C for 10 min. Fluorescently labelled MSAP products were diluted 1:10 in nanopure sterile water and 1 µl was combined with 1 µl of ROX/HiDi mix (50 µl ROX plus 1 ml of HiDiformamide, Applied Biosystems, USA). Samples were heat-denatured at 95°C for 3–5 min and snap-

bioRxiv preprint doi: https://doi.org/10.1101/059477; this version posted June 17, 2016. The copyright holder for this preprint (which was not certified by peer review) is the author/funder, who has granted bioRxiv a license to display the preprint in perpetuity. It is made available under aCC-BY-NC-ND 4.0 International license.

cooled on ice for 2 min. Samples were fractionated on an ABI PRISM 3100 at 3 kV for 22 s and at 15 kV for 45 min.

Analysis of genetic/epigenetic variability during time in culture using MSAP

MSAP profiles were visualized using GeneMapper Software v4 (Applied Biosystems, Foster City, CA). A qualitative analysis was carried out in which epiloci were scored as ‘‘present’’ (1) or ‘‘absent’’ (0) to form a presence/absence binary matrix. The selection of MSAP fragments was limited to allelic sizes between 80 and 585bp to reduce the potential impact of size homoplasy (50). Samples were grouped according to the time in culture when they were collected (1, 2, 3, 4, 5, 6, 7, 8 months and 8 months and inoculation onto *A. thaliana* called T1, T2, T3, T4, T5, T6, T7 and T7P hereafter). MSAP profile polymorphisms between DNA samples from different culture time points were considered as *in vitro* culture induced methylation differences.

Epigenetic similarity between tested samples based on profiles obtained from primer combination E2/H1 and both enzymes (*Hpa*II and *Msp*I) was first visualized using Principal Coordinate Analysis (PCoA) (51) using GenAlex (v.6.4) (52). We then used Analysis of Molecular Variance (AMOVA) (53) to evaluate the structure and degree of epigenetic diversity induced by different times in culture. Pairwise PhiPT (54) comparisons between samples restricted with *Hpa*II or *Msp*I from each time point and the samples after the first passage (2 months in culture, T1) were used to infer their overall level of divergence in DNA methylation with time in culture (i.e., the lower the PhiPT value between samples T1 restricted using *Hpa*II or *Msp*I the smaller the differentiation induced by culture and the same samples). AMOVA was subsequently calculated using GenAlex (v.6.5) to test the

bioRxiv preprint doi: https://doi.org/10.1101/059477; this version posted June 17, 2016. The copyright holder for this preprint (which was not certified by peer review) is the author/funder, who has granted bioRxiv a license to display the preprint in perpetuity. It is made available under aCC-BY-NC-ND 4.0 International license.

significance of PhiPT between populations (54), with the probability of non-differentiation (PhiPT=0) being estimated over 9,999 random permutations.

Mantle test analysis was used to estimate the correlation between the calculated pairwise genetic/epigenetic distances and the difference in virulence between culture time points. The level of significance was assigned estimated over 9,999 random permutations tests, as implemented in Genalex v6.5.

Methylation analysis by bisulphite sequencing

DNA from 9 biological replicates from culture of two different ages (1, 8 months) and from 9 replicates of tissue recovered from samples culture for eight months and the inoculated onto an *A. thaliana* plant were randomly selected for sequencing. Biological replicates were used to generate 3 pooled samples per culture age. Bisulphite treatment was performed independently from 50ng of genomic DNA of each pooled sample using the EZ DNA methylation-Gold™ Kit (Zymo Research) according to the manufacturers' instructions adjusting the final column purification elution volume to 10 µl. Following Bisulphite treatment, recovered DNA from each pool was used to estimate yield using a NanoDrop 100 spectrophotometer with the RNA setting. The remaining bisulphite treated sample were then used to create a sequencing library using the EpiGnome™ Methyl-Seq Kit (Epicentre) according to manufacturer's instructions and using EpiGnome™ Index PCR Primers (4-12).

In order to provide a reference draft sequence for the alignment of the bisulphite treated DNA and to detect any culture induced genetic variability, 10 ng of native (non-bisulphite treated) DNA extracted from 3 independent cultures from two time points (1 month (T1) and 8 month (T8)) were pooled by time point, sequenced and compared to the B. *cinerea* B05.10 genome

bioRxiv preprint doi: https://doi.org/10.1101/059477; this version posted June 17, 2016. The copyright holder for this preprint (which was not certified by peer review) is the author/funder, who has granted bioRxiv a license to display the preprint in perpetuity. It is made available under aCC-BY-NC-ND 4.0 International license.

sequence. Sequencing libraries were prepared using the EpiGnome™ Methyl-Seq Kit (Epicentre) according to manufacturer's instructions. Native DNA libraries were uniquely indexed using EpiGnome™ Index PCR Primers (Epicentre) (1-3).

Library yield was determined by Qubit dsDNA High Sensitivity Assay Kit. Agilent 2100 Bioanalyzer High-Sensitivity DNA Chip was used to assess library quality and determine average insert size. Libraries were then pooled and sequenced on Illumina HiSeq 2000 (Illumina Inc., San Diego, CA) using 100bp paired end V3 chemistry by QBI Centre for Brain Genomics.

Sequence analysis and differential methylation analysis

Obtained sequencing reads were trimmed to remove adaptors using *TrimGalore*! (http://www.bioinformatics.babraham.ac.uk/projects/trim_galore) and *Cutadapt* (55). Whole genome re-sequencing reads were aligned to the published genome from *B. cinerea* B05.10 (Broad Institute's *B. cinerea* Sequencing Project; https://www.broadinstitute.org/scientific-community/science/projects/fungal-genome-initiative/botrytis-cinerea-genome-project) using *bowtie2* (56) and variants were called using *freebayes* (57). Variant categories were analysed using *CooVar* (58), *bedtools* (59) and custom scripts. Bisulfite treated libraries were mapped using Bismark (Krueger and Andrews, 2011) and bowtie2, duplicates removed and methylation calls were extracted using samtools (60) and in-house scripts. Bisulfite sequencing efficiency was calculated by aligning reads to the B. *cinerea* mitochondrial genome scaffold (B05.10) and identifying non-bisulfite converted bases. Differentially methylated regions were called using a sliding window approach described in swDMR (https://code.google.com/p/swdmr/) using and Kruskal-Wallis (3 sample) statistical tests.

bioRxiv preprint doi: https://doi.org/10.1101/059477; this version posted June 17, 2016. The copyright holder for this preprint (which was not certified by peer review) is the author/funder, who has granted bioRxiv a license to display the preprint in perpetuity. It is made available under aCC-BY-NC-ND 4.0 International license.

Author contributions:

J.B. did sequence data analysis and helped drafting the manuscript. A.S. cultured the *Botrytis* samples and performed the virulence analysis. A.A. undertook the estimations of *in planta* fungal develop using qPCR. M.W. and L.A.J.M. helped to conceive the study and drafting the manuscript. C.M.R.L. conceived the study, carried out all nucleic acid extractions, performed and analysed the MSAPs, performed and assisted analysing the native and bisulfite treated DNA sequencing and wrote the manuscript. All authors have read and approved the final manuscript.

Acknowledgements

Janette Edson @ QBI

Bibliography

1. Fournier E, Gladieux P, Giraud T. The “Dr Jekyll and Mr Hyde fungus”: noble rot versus gray mold symptoms of Botrytis cinerea on grapes. Evol Appl. 2013 Sep;6(6):960–969.
2. Weiberg A, Wang M, Lin FM, Zhao H, Zhang Z, Kaloshian I, et al. Fungal small RNAs suppress plant immunity by hijacking host RNA interference pathways. Science. 2013 Oct 4;342(6154):118–123.
3. Martinez F, Dubos B, Fermaud M. The Role of Saprotrophy and Virulence in the Population Dynamics of Botrytis cinerea in Vineyards. Phytopathology. 2005 Jun;95(6):692–700.
4. Pathirana R, Cheah LH, Carimi F, Carra A. Low temperature stored in cryobank® maintains pathogenicity in grapevine. cryoletters [Internet]. 2009;30(1):84. Available from: http://www.cryoletters.org/Abstracts_Vol30_1pp76-88.pdf

bioRxiv preprint doi: https://doi.org/10.1101/059477; this version posted June 17, 2016. The copyright holder for this preprint (which was not certified by peer review) is the author/funder, who has granted bioRxiv a license to display the preprint in perpetuity. It is made available under aCC-BY-NC-ND 4.0 International license.

5. Butt T, Wang C, Shah F, Hall R. DEGENERATION OF ENTOMOGENOUS FUNGI. In: EILENBERG J, HOKKANEN H, editors. An Ecological and Societal Approach to Biological Control. Dordrecht: Springer Netherlands; 2006. p. 213–226.

6. Castro M, Kramer K, Valdivia L, Ortiz S, Castillo A. A double-stranded RNA mycovirus confers hypovirulence-associated traits to Botrytis cinerea. FEMS Microbiol Lett. 2003 Nov 7;228(1):87–91.

7. Chu YM, Jeon JJ, Yea SJ, Kim YH, Yun SH, Lee YW, et al. Double-stranded RNA mycovirus from Fusarium graminearum. Appl Environ Microbiol. 2002 May;68(5):2529–2534.

8. Hatta R, Ito K, Hosaki Y, Tanaka T, Tanaka A, Yamamoto M, et al. A conditionally dispensable chromosome controls host-specific pathogenicity in the fungal plant pathogen Alternaria alternata. Genetics. 2002 May;161(1):59–70.

9. Akamatsu H, Taga M, Kodama M, Johnson R, Otani H, Kohmoto K. Molecular karyotypes for Alternaria plant pathogens known to produce host-specific toxins. Curr Genet. 1999 Jul;35(6):647–656.

10. Kelly SA, Panhuis TM, Stoehr AM. Phenotypic plasticity: molecular mechanisms and adaptive significance. Compr Physiol. 2012 Apr;2(2):1417–1439.

11. WADDINGTON C. Canalization of Development and the Inheritance of Acquired Characters. Nature. 1942 Nov 14;150(3811):563–565.

12. Tricker PJ, Gibbings JG, Rodríguez López CM, Hadley P, Wilkinson MJ. Low relative humidity triggers RNA-directed de novo DNA methylation and suppression of genes controlling stomatal development. J Exp Bot. 2012 Jun;63(10):3799–3813.

13. Geyer KK, Rodríguez López CM, Chalmers IW, Munshi SE, Truscott M, Heald J, et al. Cytosine methylation regulates oviposition in the pathogenic blood fluke Schistosoma mansoni. Nat Commun. 2011 Aug 9;2:424.

14. Bird A. Perceptions of epigenetics. Nature. 2007 May 24;447(7143):396–398.

15. Rodríguez López CM, Wilkinson MJ. Epi-fingerprinting and epi-interventions for improved crop production and food quality. Front Plant Sci. 2015 Jun 5;6:397.

16. Su Z, Han L, Zhao Z. Conservation and divergence of DNA methylation in eukaryotes: new insights from single base-resolution DNA methylomes. Epigenetics. 2011 Feb 1;6(2):134–140.

17. He XJ, Chen T, Zhu JK. Regulation and function of DNA methylation in plants and animals. Cell Res. 2011 Mar;21(3):442–465.

18. Jupe ER, Magill JM, Magill CW. Stage-specific DNA methylation in a fungal plant pathogen. J Bacteriol. 1986 Feb;165(2):420–423.

bioRxiv preprint doi: https://doi.org/10.1101/059477; this version posted June 17, 2016. The copyright holder for this preprint (which was not certified by peer review) is the author/funder, who has granted bioRxiv a license to display the preprint in perpetuity. It is made available under aCC-BY-NC-ND 4.0 International license.

19. Jeon J, Choi J, Lee GW, Park SY, Huh A, Dean RA, et al. Genome-wide profiling of DNA methylation provides insights into epigenetic regulation of fungal development in a plant pathogenic fungus, Magnaporthe oryzae. Sci Rep. 2015 Feb 24;5:8567.

20. Armaleo D, Miao V. Symbiosis and DNA methylation in the Cladonia lichen fungus. Symbiosis [Internet]. 1999;26(2):143 – 163. Available from: https://scholars.duke.edu/display/pub758042

21. Zemach A, McDaniel IE, Silva P, Zilberman D. Genome-wide evolutionary analysis of eukaryotic DNA methylation. Science. 2010 May 14;328(5980):916–919.

22. Boyko A, Kovalchuk I. Genetic and epigenetic effects of plant-pathogen interactions: an evolutionary perspective. Mol Plant. 2011 Nov;4(6):1014–1023.

23. Reyna-López GE, Simpson J, Ruiz-Herrera J. Differences in DNA methylation patterns are detectable during the dimorphic transition of fungi by amplification of restriction polymorphisms. Mol Gen Genet. 1997 Feb 27;253(6):703–710.

24. Gachon C, Saindrenan P. Real-time PCR monitoring of fungal development in Arabidopsis thaliana infected by Alternaria brassicicola and Botrytis cinerea. Plant Physiol Biochem. 2004 May;42(5):367–371.

25. Jeon J, Choi J, Lee GW, Dean RA, Lee YH. Experimental evolution reveals genome-wide spectrum and dynamics of mutations in the rice blast fungus, Magnaporthe oryzae. PLoS ONE. 2013 May 31;8(5):e65416.

26. Amselem J, Cuomo CA, van Kan JA, Viaud M, Benito EP, Couloux A, et al. Genomic analysis of the necrotrophic fungal pathogens Sclerotinia sclerotiorum and Botrytis cinerea. PLoS Genet. 2011 Aug 18;7(8):e1002230.

27. Choquer M, Fournier E, Kunz C, Levis C, Pradier JM, Simon A, et al. Botrytis cinerea virulence factors: new insights into a necrotrophic and polyphageous pathogen. FEMS Microbiol Lett. 2007 Dec;277(1):1–10.

28. Blanco-Ulate B, Morales-Cruz A, Amrine KC, Labavitch JM, Powell AL, Cantu D. Genome-wide transcriptional profiling of Botrytis cinerea genes targeting plant cell walls during infections of different hosts. Front Plant Sci. 2014 Sep 3;5:435.

29. Rodríguez López CM, Wetten AC, Wilkinson MJ. Progressive erosion of genetic and epigenetic variation in callus-derived cocoa (Theobroma cacao) plants. New Phytol. 2010 Jun;186(4):856–868.

30. Dahmen H, Staub T, Schwinn FJ. Technique for Long-Term Preservation of Phytopathogenic Fungi in Liquid Nitrogen. Phytopathology. 1983;73(2):241.

31. Lombard V, Golaconda Ramulu H, Drula E, Coutinho PM, Henrissat B. The carbohydrate-active enzymes database (CAZy) in 2013. Nucleic Acids Res. 2014 Jan;42(Database issue):D490–D495.

bioRxiv preprint doi: https://doi.org/10.1101/059477; this version posted June 17, 2016. The copyright holder for this preprint (which was not certified by peer review) is the author/funder, who has granted bioRxiv a license to display the preprint in perpetuity. It is made available under aCC-BY-NC-ND 4.0 International license.

32. Feng S, Cokus SJ, Zhang X, Chen PY, Bostick M, Goll MG, et al. Conservation and divergence of methylation patterning in plants and animals. Proc Natl Acad Sci U S A. 2010 May 11;107(19):8689–8694.

33. Jung M, Pfeifer GP. Aging and DNA methylation. BMC Biol. 2015 Jan 31;13:7.

34. Gómez-Díaz E, Jordà M, Peinado MA, Rivero A. Epigenetics of host-pathogen interactions: the road ahead and the road behind. PLoS Pathog. 2012 Nov 29;8(11):e1003007.

35. Cheeseman K, Weitzman JB. Host-parasite interactions: an intimate epigenetic relationship. Cell Microbiol. 2015 Aug;17(8):1121–1132.

36. Hervouet E, Cheray M, Vallette FM, Cartron PF. DNA methylation and apoptosis resistance in cancer cells. Cells. 2013 Jul 18;2(3):545–573.

37. Belden WJ, Lewis ZA, Selker EU, Loros JJ, Dunlap JC. CHD1 remodels chromatin and influences transient DNA methylation at the clock gene frequency. PLoS Genet. 2011 Jul 21;7(7):e1002166.

38. Montanini B, Chen PY, Morselli M, Jaroszewicz A, Lopez D, Martin F, et al. Non-exhaustive DNA methylation-mediated transposon silencing in the black truffle genome, a complex fungal genome with massive repeat element content. Genome Biol. 2014 Jul 31;15(7):411.

39. Mishra PK, Baum M, Carbon J. DNA methylation regulates phenotype-dependent transcriptional activity in Candida albicans. Proc Natl Acad Sci U S A. 2011 Jul 19;108(29):11965–11970.

40. Veneault-Fourrey C, Martin F. Mutualistic interactions on a knife-edge between saprotrophy and pathogenesis. Curr Opin Plant Biol. 2011 Aug;14(4):444–450.

41. Consuegra del Olmo S, Rodriguez Lopez CM. Epigenetic-induced alterations in sex-ratios in response to climate change: an epigenetic trap? BioEssays.

42. O'Dea RE, Noble DWA, Johnson SL, Hesselson D, Nakagawa S. The role of non-genetic inheritance in evolutionary rescue: epigenetic buffering, heritable bet hedging and epigenetic traps. Environmental epigenetics. 2016;2(1):dvv014.

43. Thomma BP, Eggermont K, Tierens KF, Broekaert WF. Requirement of functional ethylene-insensitive 2 gene for efficient resistance of Arabidopsis to infection by Botrytis cinerea. Plant Physiol. 1999 Dec;121(4):1093–1102.

44. Johnson H, Lloyd A, Mur L, Smith A, Causton D. The application of MANOVA to analyse Arabidopsis thaliana metabolomic data from factorially designed experiments. Metabolomics. 2007 Nov 7;3(4):517–530.

bioRxiv preprint doi: https://doi.org/10.1101/059477; this version posted June 17, 2016. The copyright holder for this preprint (which was not certified by peer review) is the author/funder, who has granted bioRxiv a license to display the preprint in perpetuity. It is made available under aCC-BY-NC-ND 4.0 International license.

45. Boyes DC, Zayed AM, Ascenzi R, McCaskill AJ, Hoffman NE, Davis KR, et al. Growth stage-based phenotypic analysis of Arabidopsis: a model for high throughput functional genomics in plants. Plant Cell. 2001 Jul;13(7):1499–1510.

46. Johnson H, Broadhurst D, Goodacre R, Smith A. Metabolic fingerprinting of salt-stressed tomatoes. Phytochemistry. 2003 Mar;62(6):919–928.

47. Lloyd AJ, William Allwood J, Winder CL, Dunn WB, Heald JK, Cristescu SM, et al. Metabolomic approaches reveal that cell wall modifications play a major role in ethylene-mediated resistance against Botrytis cinerea. Plant J. 2011 Sep;67(5):852–868.

48. Róis AS, Rodríguez López CM, Cortinhas A, Erben M, Espírito-Santo D, Wilkinson MJ, et al. Epigenetic rather than genetic factors may explain phenotypic divergence between coastal populations of diploid and tetraploid Limonium spp. (Plumbaginaceae) in Portugal. BMC Plant Biol. 2013 Dec 6;13:205.

49. Rodríguez López C, Morán P, Lago F, Espiñeira M, Beckmann M, Consuegra S. Detection and quantification of tissue of origin in salmon and veal products using methylation sensitive AFLPs. Food Chem. 2012 Apr;131(4):1493–1498.

50. Caballero A, Quesada H, Rolán-Alvarez E. Impact of amplified fragment length polymorphism size homoplasy on the estimation of population genetic diversity and the detection of selective loci. Genetics. 2008 May;179(1):539–554.

51. Gower JC. Some Distance Properties of Latent Root and Vector Methods Used in Multivariate Analysis. Biometrika [Internet]. 1966 Dec; Available from: http://www.jstor.org/stable/2333639

52. Peakall R, Smouse PE. GenAlEx 6.5: genetic analysis in Excel. Population genetic software for teaching and research--an update. Bioinformatics. 2012 Oct 1;28(19):2537–2539.

53. Excoffier L, Smouse PE, Quattro JM. Analysis of molecular variance inferred from metric distances among DNA haplotypes: application to human mitochondrial DNA restriction data. Genetics. 1992 Jun;131(2):479–491.

54. Michalakis Y, Excoffier L. A generic estimation of population subdivision using distances between alleles with special reference for microsatellite loci. Genetics. 1996 Mar;142(3):1061–1064.

55. Martin M. Cutadapt removes adapter sequences from high-throughput sequencing reads. EMBnet.journal. 2011 May 2;17(1):10.

56. Langmead B, Salzberg SL. Fast gapped-read alignment with Bowtie 2. Nat Methods. 2012 Apr;9(4):357–359.

57. Garrison E, Marth G. Haplotype-based variant detection from short-read sequencing. 2012 Jul 17; Available from: https://arxiv.org/abs/1207.3907

bioRxiv preprint doi: https://doi.org/10.1101/059477; this version posted June 17, 2016. The copyright holder for this preprint (which was not certified by peer review) is the author/funder, who has granted bioRxiv a license to display the preprint in perpetuity. It is made available under aCC-BY-NC-ND 4.0 International license.

58. Vergara IA, Frech C, Chen N. CooVar: co-occurring variant analyzer. BMC Res Notes. 2012 Nov 1;5:615.

59. Quinlan AR, Hall IM. BEDTools: a flexible suite of utilities for comparing genomic features. Bioinformatics. 2010 Mar 15;26(6):841–842.

60. Li H, Handsaker B, Wysoker A, Fennell T, Ruan J, Homer N, et al. The Sequence Alignment/Map format and SAMtools. Bioinformatics. 2009 Aug 15;25(16):2078–2079.

bioRxiv preprint doi: https://doi.org/10.1101/059477; this version posted June 17, 2016. The copyright holder for this preprint (which was not certified by peer review) is the author/funder, who has granted bioRxiv a license to display the preprint in perpetuity. It is made available under aCC-BY-NC-ND 4.0 International license.

FIGUREs AND TABLES

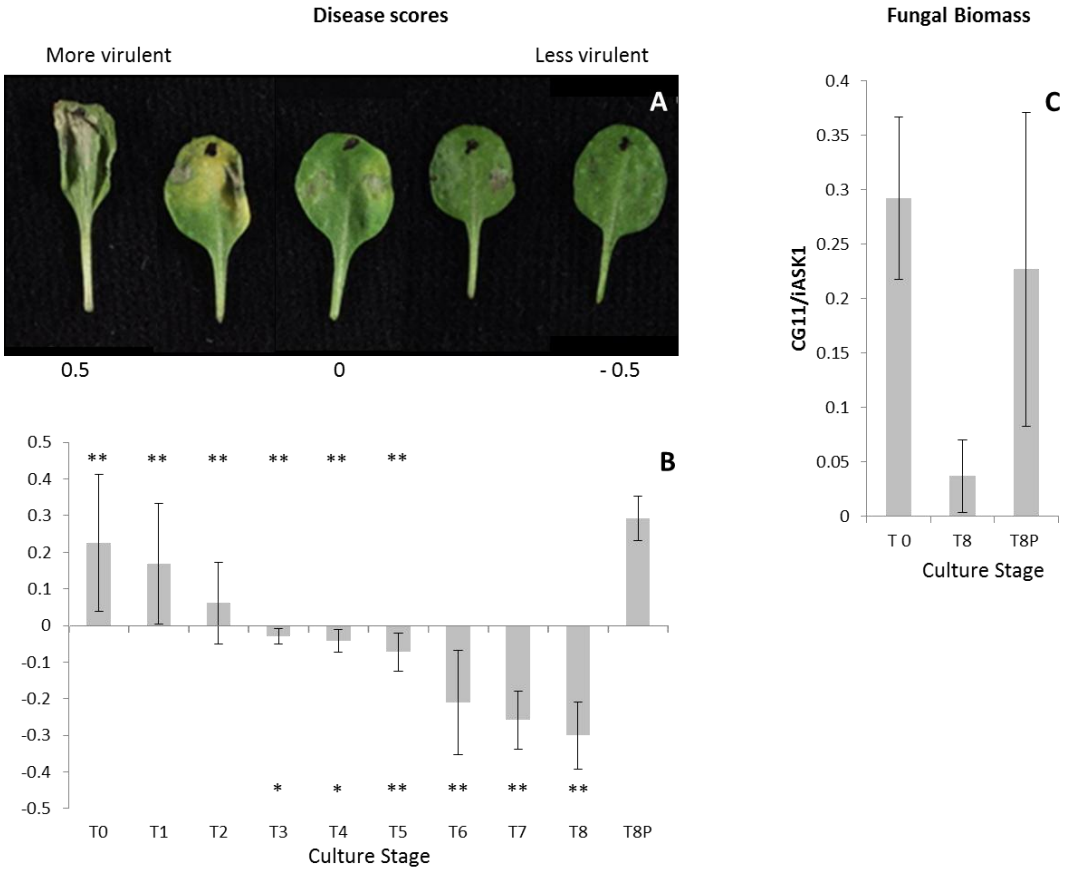

Figure 1: Estimation of *Botrytis cinerea* virulence on *Arabidopsis thaliana*. (a) Examples of *A. thaliana* Col-0 leaves drop inoculated with *B. cinerea* and presenting disease scores ranging from -0.5 (low virulence) to 0.5 (high virulence). **(b)** Estimated *B. cinerea* virulence at each time culture point. Virulence of *B. cinerea* cultures was estimated over a period of eight months in culture (T0, initial inoculum; T8, eight months in culture) and after 8 months in culture and a single passage on *A. thaliana* (T8P). A weighted scoring method was used to categorize *B. cinerea* lesion phenotypes 3 days post inoculation. Virulence symptoms (water-soaking, chlorosis, and spreading necrosis) were conferred a range of positive scores and the

bioRxiv preprint doi: https://doi.org/10.1101/059477; this version posted June 17, 2016. The copyright holder for this preprint (which was not certified by peer review) is the author/funder, who has granted bioRxiv a license to display the preprint in perpetuity. It is made available under aCC-BY-NC-ND 4.0 International license.

resistant symptoms (necrosis limited to inoculation site) were given negative scores. Asterisk symbols under the horizontal axis indicate significant differences (*(T-Test; P< 0.05) and ** (T-Test; P< 0.01)) between T0 and the time point over the asterisk. Asterisk symbols over the horizontal axis indicate significant differences (** (T-Test; P< 0.01)) between T8P and the time point under the asterisk. **(c)** Detection of *in planta B. cinerea* hyphal mass in *A. thaliana* Col-0 by qPCR as described by Gachon and Saindrenan, 2004.

bioRxiv preprint doi: https://doi.org/10.1101/059477; this version posted June 17, 2016. The copyright holder for this preprint (which was not certified by peer review) is the author/funder, who has granted bioRxiv a license to display the preprint in perpetuity. It is made available under aCC-BY-NC-ND 4.0 International license.

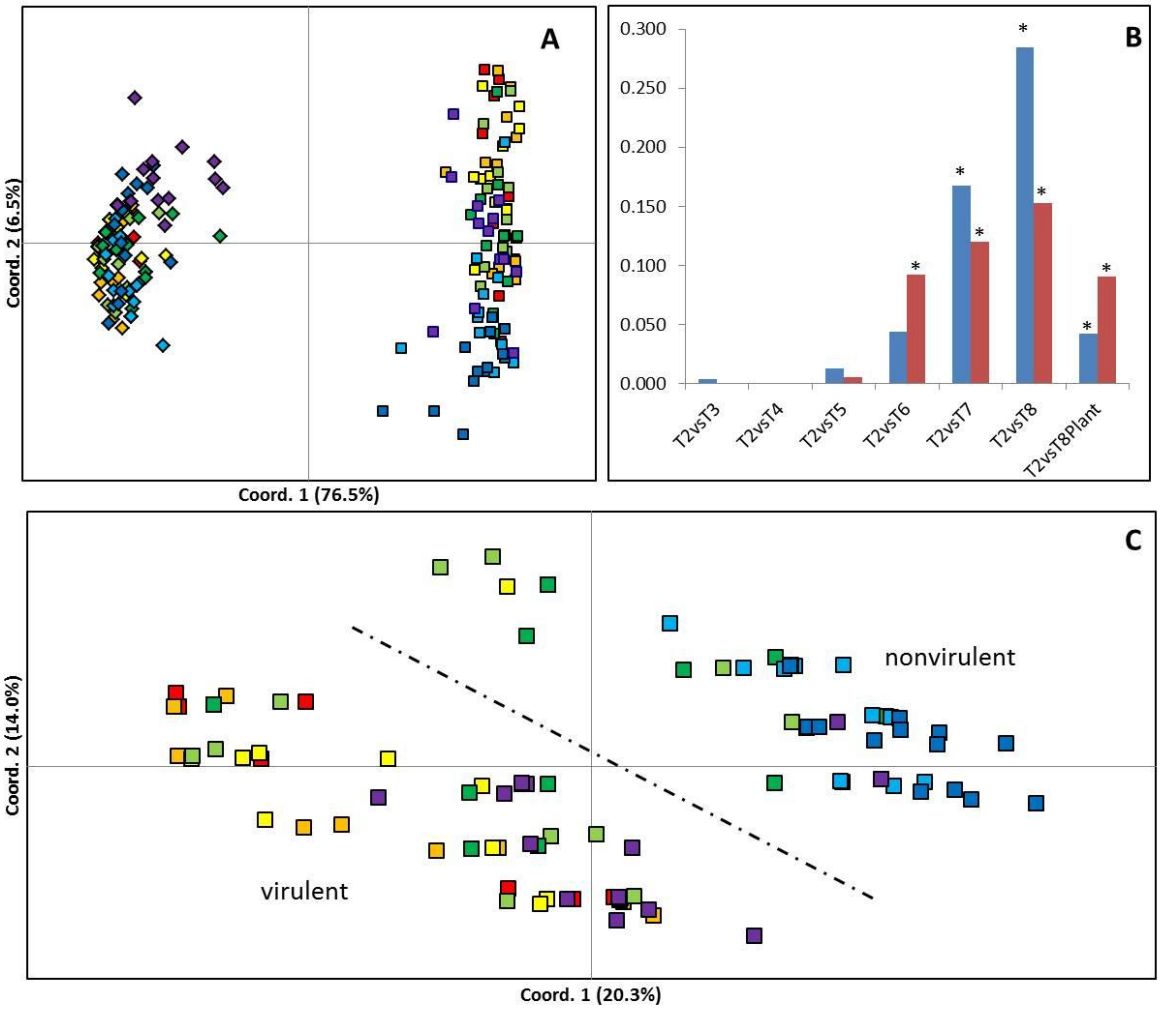

Figure 2: Effect of time in culture on genetic/epigenetic instability. (a, c) Principal coordinate diagrams based on the Euclidian analysis of methylation-sensitive amplified polymorphisms (MSAP) using enzymes *Hpa*II (squares) and *Msp*I (romboids) **(a)** and using enzyme *Hpa*II distances **(c)**. 14 replicates from each time point are represented as red (T2: 2 months in culture), orange (T3: 3 months in culture), yellow (T4: 4 months in culture), light green (T5: 5 months in culture), dark green (T6: 6 months in culture), light blue (T7: 7 months in culture), dark blue (T8: 8 months in culture), and purple (T8P: 8 months+plant). The dashed line separates samples with higher average levels of virulence from those of lower average levels of virulence. **(b)** Calculated Pairwise PhiPT (Michalakis & Excoffier, 1996) comparisons between samples restricted with *Hpa*II (Blue) or *Msp*I (Red) from each

bioRxiv preprint doi: https://doi.org/10.1101/059477; this version posted June 17, 2016. The copyright holder for this preprint (which was not certified by peer review) is the author/funder, who has granted bioRxiv a license to display the preprint in perpetuity. It is made available under aCC-BY-NC-ND 4.0 International license.

time point and the samples after the second passage (2 months in culture). * Indicates significantly different PhiPT values between T1 and the time point under the asterix based on 10,000 permutations (Probability values > 0.05).

bioRxiv preprint doi: https://doi.org/10.1101/059477; this version posted June 17, 2016. The copyright holder for this preprint (which was not certified by peer review) is the author/funder, who has granted bioRxiv a license to display the preprint in perpetuity. It is made available under aCC-BY-NC-ND 4.0 International license.

838

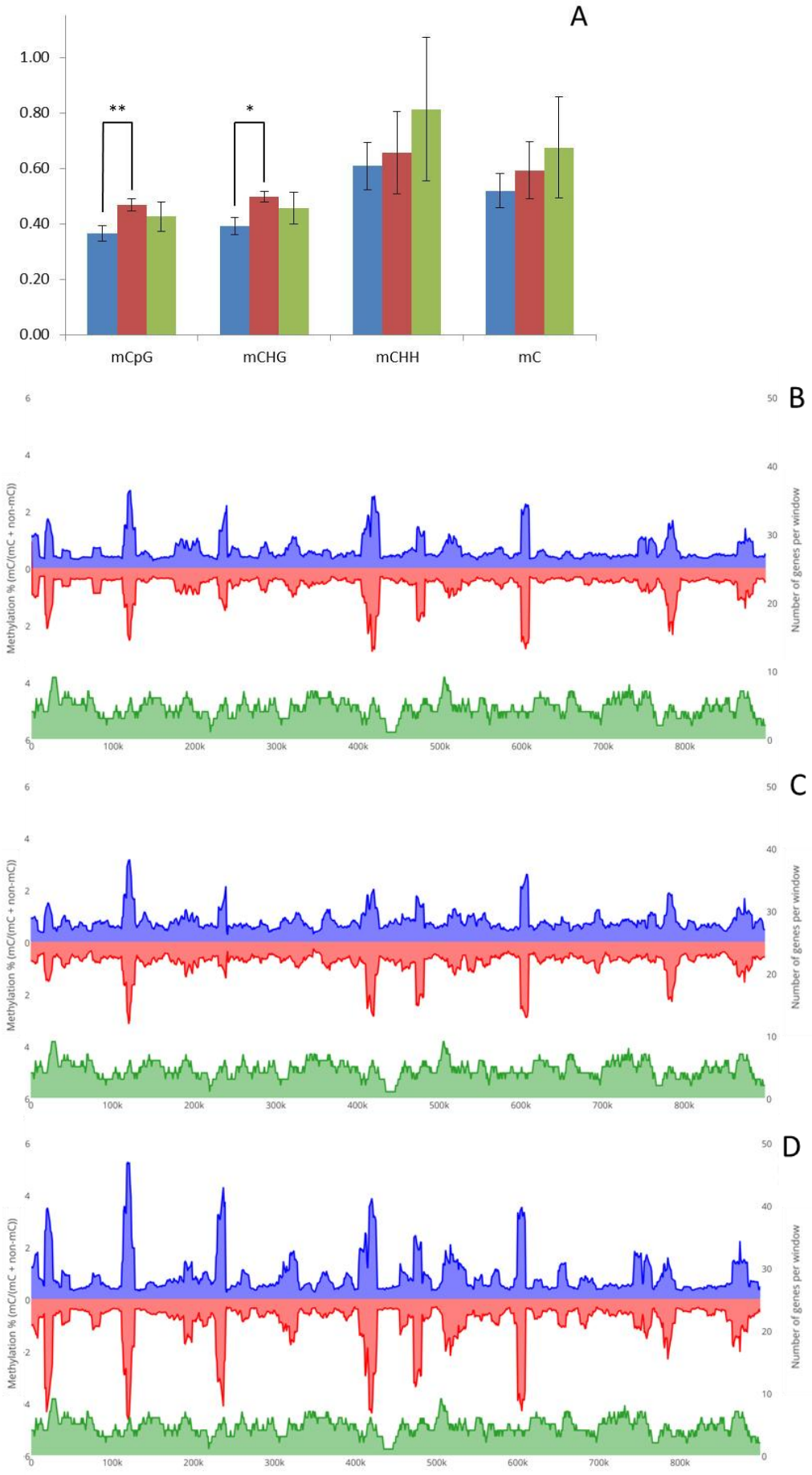

839

bioRxiv preprint doi: https://doi.org/10.1101/059477; this version posted June 17, 2016. The copyright holder for this preprint (which was not certified by peer review) is the author/funder, who has granted bioRxiv a license to display the preprint in perpetuity. It is made available under aCC-BY-NC-ND 4.0 International license.

Figure 3. Global changes on genomic distribution and levels of DNA methylation in B. cinerea. A) Global average proportions of mCs (number of mCs/total Cs) at each time point (T1, Blue; T8, red and T8P, green). **B-D)** Methylcytosines (mCs) density from each strand (blue, positive and red, negative strand) across supercontig 1.1 at each time point (**B**=T0; **C**=T8 and **D**=T8P) was calculated and plotted as the proportion of methylated cytosines (mCs/total Cs) in each 10kb window.

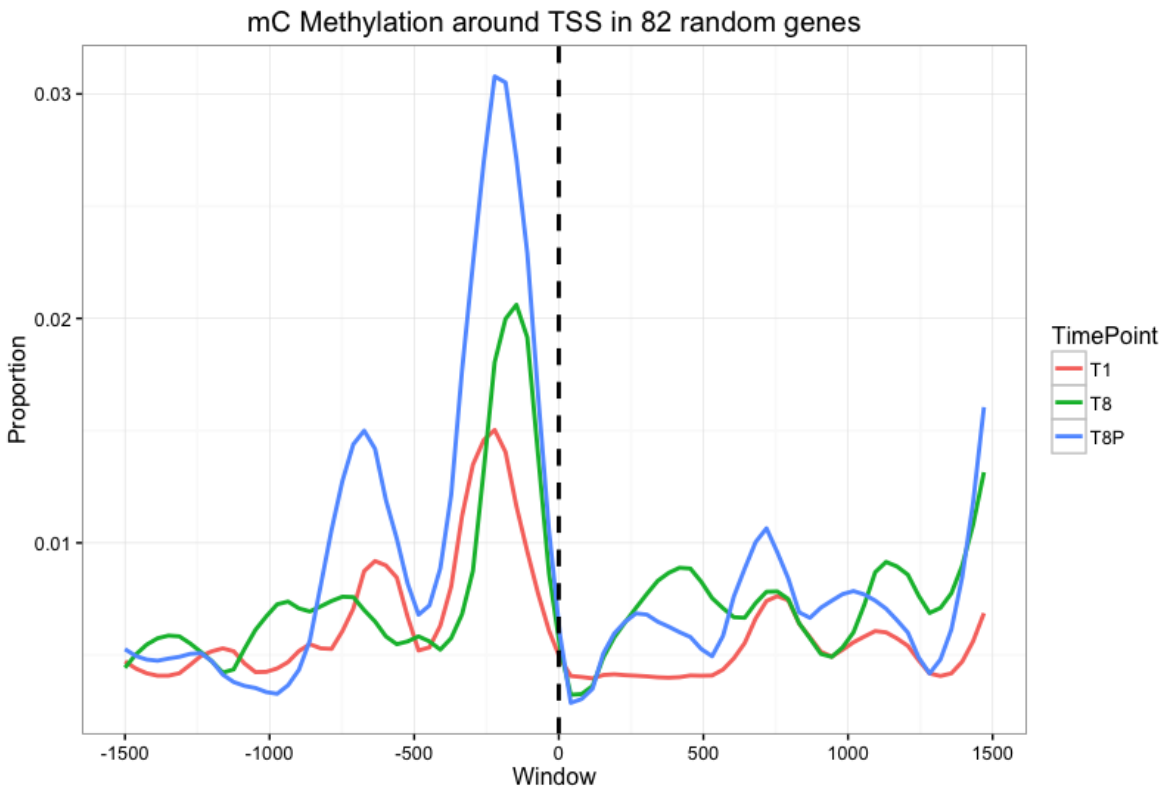

Figure 4: Methylation density across transcription start sites (TSS) found in 82 randomly selected genes. Methylation density was identified by the proportion of methyl cytosine's against all cytosine's in 30bp windows 1.5kb before and after the transcription start site.

bioRxiv preprint doi: https://doi.org/10.1101/059477; this version posted June 17, 2016. The copyright holder for this preprint (which was not certified by peer review) is the author/funder, who has granted bioRxiv a license to display the preprint in perpetuity. It is made available under aCC-BY-NC-ND 4.0 International license.

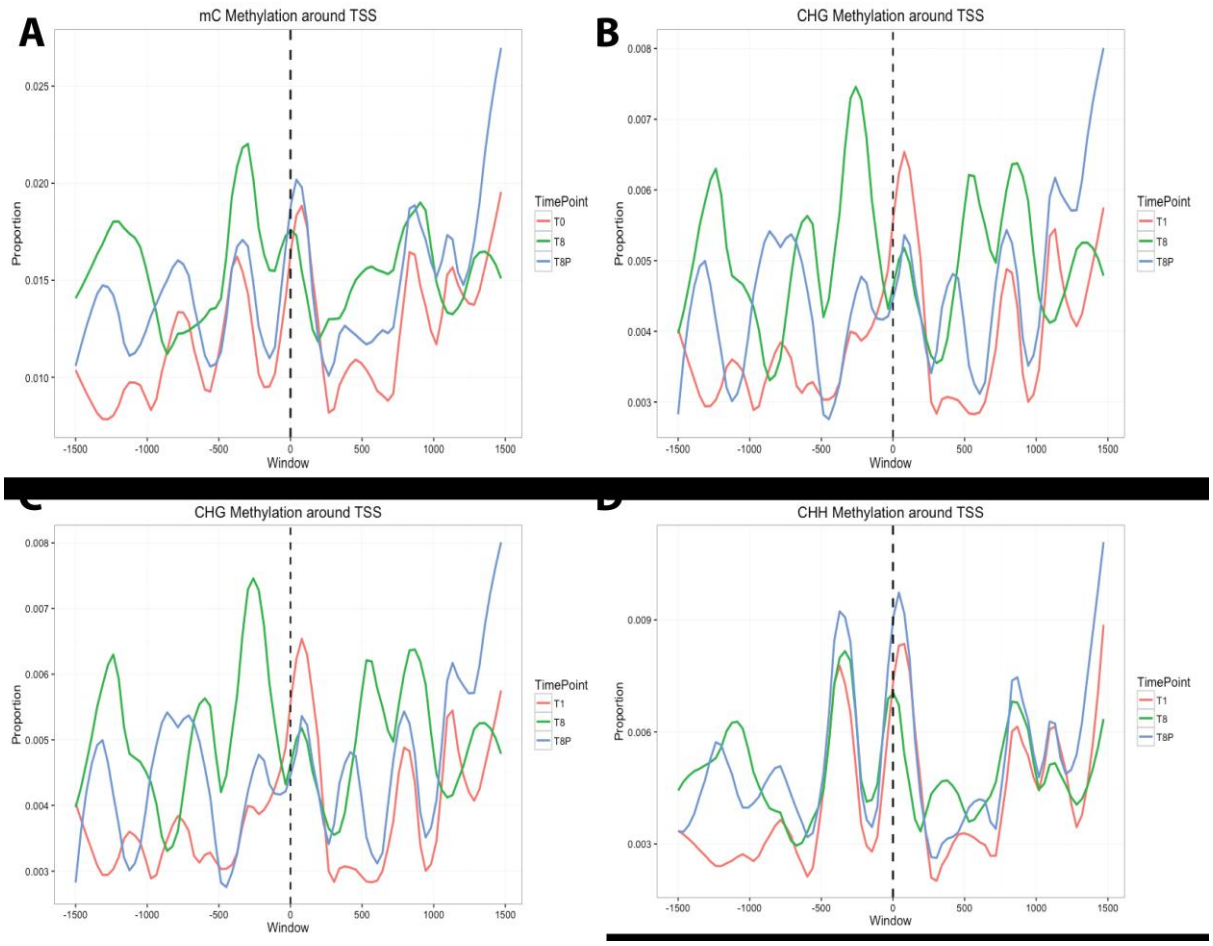

Figure 5: Methylation density across transcription start sites (TSS) found in 121 genes associated to polysaccharide degradation in *B. cinerea* (27) at each time point (T1, Blue; T8, red and T8P, green). Methylation level (Vertical axis) was identified by the proportion of methyl cytosine's against all cytosine's in 30bp windows 1.5kb before and after the transcription start site (TSS) (Horizontal axis). **A)** Methylation level for all mCs; **B)** Methylation level for CpG context; **C)** Methylation level for CpHpG context and **D)** Methylation level for CpHpH context.

bioRxiv preprint doi: https://doi.org/10.1101/059477; this version posted June 17, 2016. The copyright holder for this preprint (which was not certified by peer review) is the author/funder, who has granted bioRxiv a license to display the preprint in perpetuity. It is made available under aCC-BY-NC-ND 4.0 International license.

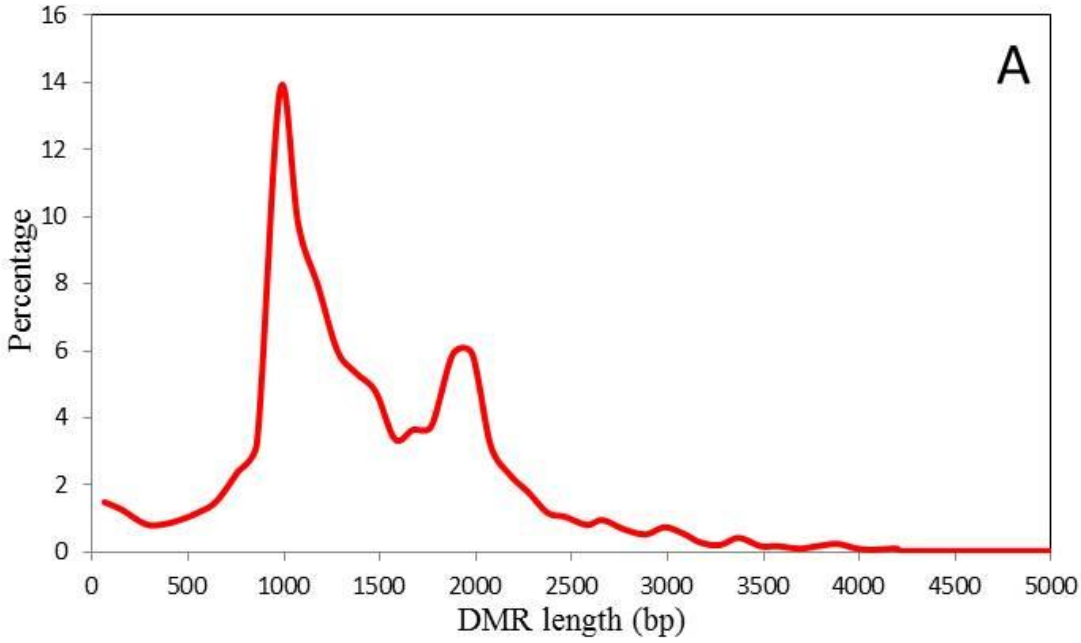

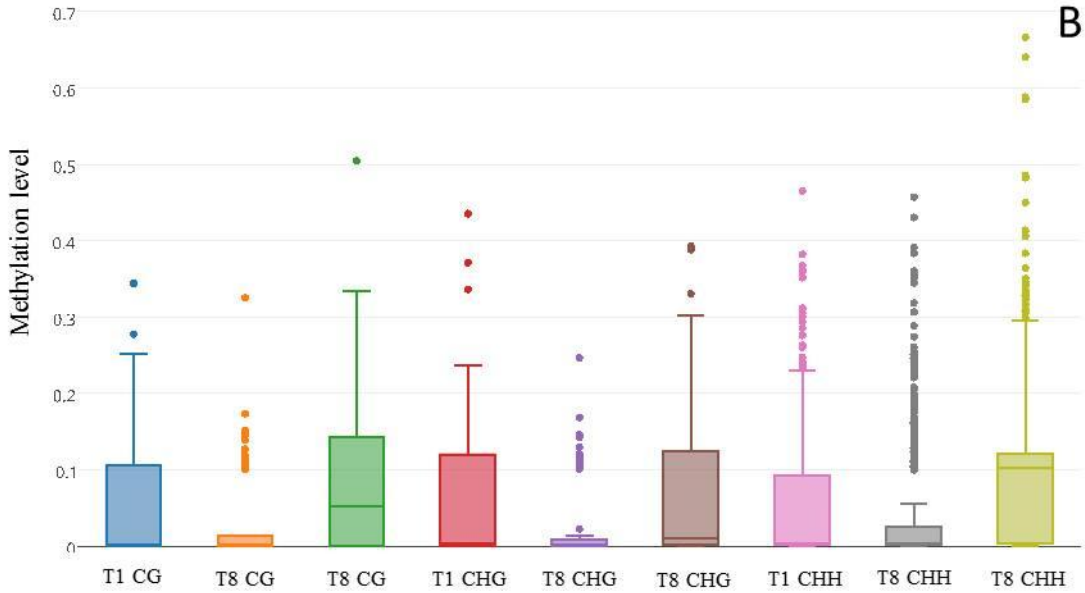

Figure 6: Analysis of *in vitro* culture induced DMRs in *Botrytis cinerea*. (a) Length distribution of *in vitro* culture induced DMRs in *Botrytis cinerea*. DRMs (i.e., regions presenting significantly different methylation levels between one sample and the other two samples (FDR<0.01)) were determined using a three sample Kruskal-Wallis test. Methylation levels were analysed by sliding window analysis using swDMR. DMRs were determined for all cytosines. **(b)** Methylation level distribution in *in vitro* induced DMRs. Boxplot of 3 sample sliding window differential methylation analysis using swDMR. The boxplots shows

bioRxiv preprint doi: https://doi.org/10.1101/059477; this version posted June 17, 2016. The copyright holder for this preprint (which was not certified by peer review) is the author/funder, who has granted bioRxiv a license to display the preprint in perpetuity. It is made available under aCC-BY-NC-ND 4.0 International license.

the distribution of each methylation in each context (CG, CHG and CHH) at three time points (T1, T8 and T8P), circles indicate DMRs with outlier levels of methylation.

bioRxiv preprint doi: https://doi.org/10.1101/059477; this version posted June 17, 2016. The copyright holder for this preprint (which was not certified by peer review) is the author/funder, who has granted bioRxiv a license to display the preprint in perpetuity. It is made available under aCC-BY-NC-ND 4.0 International license.

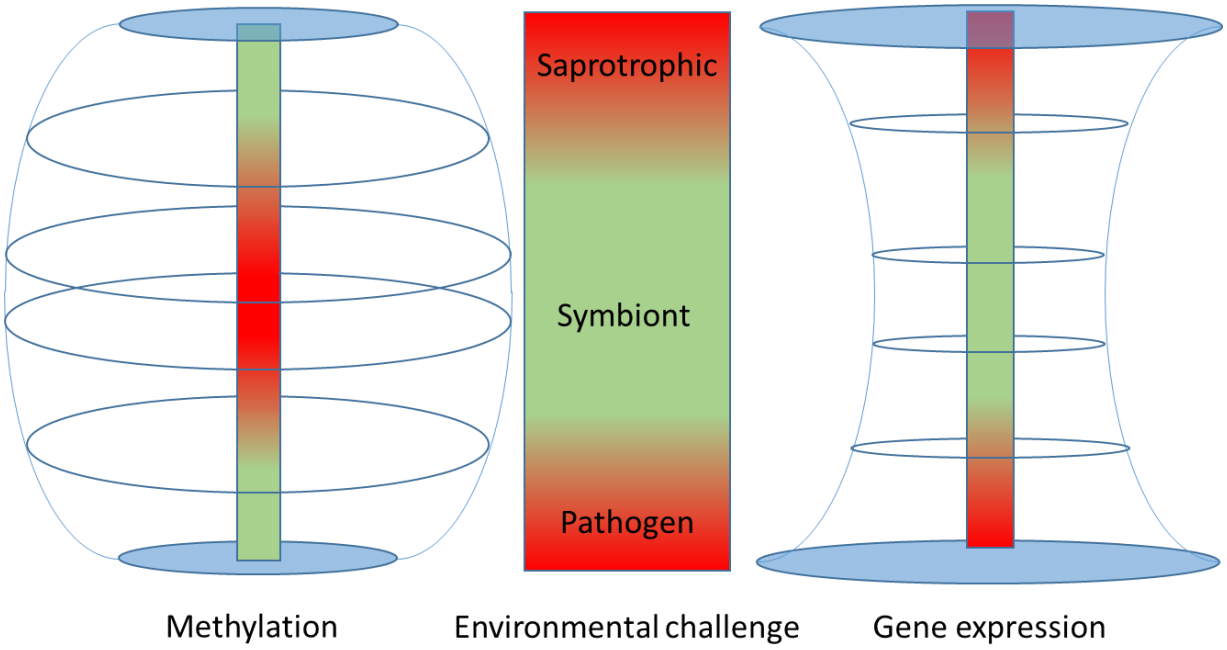

Figure 7. Effect of level of environmental challenge on the number of expressed genes and DNA methylation level on the fungal life style continuum: DNA methylation follows a barrel model with lichen fungi and *ectomycorrhizae* (confronted with stable environments provided by their hosts) presenting higher global levels of DNA methylation compared to their saprotrophic free living form (FLF). Conversely pathogenic fungi face a more challenging environment when infecting a host than their free living forms. Since DNA methylation is indicative of lower levels of gene expression the predicted number of gene expresses should follow a 'hourglass' model with free living fungal species saprotrophic and pathogenic, presenting a higher number of genes expressed to survive the more challenging environments. Red shading indicates higher levels of DNA methylation, number of expressed genes and environmental challenge. Green shading represent low levels of the same parameters.

bioRxiv preprint doi: https://doi.org/10.1101/059477; this version posted June 17, 2016. The copyright holder for this preprint (which was not certified by peer review) is the author/funder, who has granted bioRxiv a license to display the preprint in perpetuity. It is made available under aCC-BY-NC-ND 4.0 International license.

Table 1: *Botrytis cinerea* virulence genes overlapping with *in vitro* culture induced DMRs. Column DRM overlap/context/pattern indicates what region of the gene overlaps with the DRM (P= promoter; G= Gene body; 3' after downstream of the 3'UTR) in what Cytosine context the DMR is observed (mC= all Cytosines; CG, CHG and CHH) what DNA methylation behaviour the DMR showed when comparing all three samples (2, T1=T8P > T8; 1a, T1>T8=T8P; 1b, T1=T8<T8P and 0, T1=T8P < T8). (1,2)(1,2)(26,27)(1,2)(1,2)

Gene Function		Total			Gene/DMR Overlap		DMR Type				Reference
			#G/D	%G/D	#G/D	%G/D	recovery		Non-recov		
							0	2	1a	1b	
Housekeeping		5	-	-	-	-	-	-	-	-	(26)
Apoptosis		10	2	20	4	40.0	3	1	-	-	(26)
Conidiation		16	-	-	6	37.5	1	2	-	3	(26)
Mating and fruit body development		32	6	18.8	6	18.7	1	4	1	1	(26)
Secondary metabolism		51	4	7.8	14	27.5	9	3	2	3	(26)
Signalling pathways		176	6	3.4	54	30.7	12	17	7	20	(26)
Sclerotium formation		249	7	2.8	67	26.9	26	31	10	13	(26)
Virul. *s.l.*	Appressorium	12	2	16.7	3	25.0	1	-	-	3	(26)
	Virulence *s.s.*	17	1	5.9	4	23.5	1	1	1	2	(27)
	CAZyme genes	1155	50	4.3	320	27.7	112	132	45	99	(28)
Total		**1577**	**68**	**4.3**	**478**	**30.3**	**166**	**191**	**66**	**144**	

bioRxiv preprint doi: https://doi.org/10.1101/059477; this version posted June 17, 2016. The copyright holder for this preprint (which was not certified by peer review) is the author/funder, who has granted bioRxiv a license to display the preprint in perpetuity. It is made available under aCC-BY-NC-ND 4.0 International license.

Table 2: Coverage statistics for bisulfite samples

Sample	Mean Coverage	Std dev	Cytosine coverage	Cytosine coverage (>4x)	mC (>1x)
T1	54.9939	20.3428	92.55%	87.65%	10.99%
T8	33.1991	13.868	91.50%	81.07%	9.14%
T8P	45.0209	17.0144	93.42%	86.67%	10.63%

bioRxiv preprint doi: https://doi.org/10.1101/059477; this version posted June 17, 2016. The copyright holder for this preprint (which was not certified by peer review) is the author/funder, who has granted bioRxiv a license to display the preprint in perpetuity. It is made available under aCC-BY-NC-ND 4.0 International license.

Table 2: Number of Differentially Methylated Regions (DMRs) between T1, T8 and T8P samples. DRMs (i.e., regions presenting significantly different methylation levels between one sample and the other two samples (FDR<0.01)) were determined using a three sample Kruskal-Wallis test. Methylation levels were analysed by sliding window analysis using swDMR. DMRs were determined for all cytosines and for three methylation contexts. DMRs were grouped according to their changing patterns into recovery (T1=T8P) and non-recovery (T1< > T8P). Two subgroups where found for recovery (T1=T8P < T8 (Type 0) and T1=T8P > T8 (Type 2)) and non-recovery (T1>T8=T8P (Type 1a) and T1=T8<T8P (Type 1b)). Percentage of the total DMRs for each pattern type/sequence context is shown in parenthesis.

	Total	Recovery (%)		Total recovery (%)	No recovery	
		Type 0	Type 2		In vitro induced (Type 1a)	Plant induced (Type 1b)
mC	2822	757 (26.82)	860 (30.47)	1617 (57.30)	452 (16.02)	753 (26.68)
CG	70	17 (24.29)	15 (21.43)	32 (45.71)	14 (20.00)	24 (34.29)
CHG	82	14 (17.07)	30 (36.59)	44 (53.66)	15 (18.29)	23 (28.05)
CHH	1248	303 (24.28)	490 (39.26)	793 (63.54)	137 (10.98))	318 (25.48)
Total	4222	1395 (33.04)	1091 (25.84)	2486(58.88)	618 (14.64)	1118 (26.48)

bioRxiv preprint doi: https://doi.org/10.1101/059477; this version posted June 17, 2016. The copyright holder for this preprint (which was not certified by peer review) is the author/funder, who has granted bioRxiv a license to display the preprint in perpetuity. It is made available under aCC-BY-NC-ND 4.0 International license.

Table 3: *Botrytis cinerea in vitro* induced Differentially Methylated Regions overlapping with genes. DRMs overlapping with genes (i.e., regions presenting significantly different methylation levels between one sample and the other two samples (FDR<0.01)) were determined using a three sample Kruskal-Wallis test. Methylation levels were analyzed by sliding window analysis using swDMR. DMRs were determined for all cytosines and for three methylation contexts. DMRs were grouped according to the genic region they overlapped with (i.e, Promoter, promoter and Gene body, promoter, Gene body and 3'UTR, gene body and 3'UTR and gene body). (**) Percentage of the total DMRs overlapping with each particular genic region. (*) Percentage of the total number of genes showing a methylation recovery pattern.

	Total genes	Promoter, Gene body and 3'UTR (*)	Promoter only (*)	Promoter and Gene body (*)	Gene body and 3'UTR (*)	Gene body (*)
mC	3055	626 (20.49)	61 (2.00)	1022 (33.45)	923 (30.21)	423 (13.85)
CG	68	3 (4.41)	0 (0.00)	24 (35.29)	21 (30.88)	20 (29.41)
CHG	84	8 (9.52)	0 (0.00)	29 (34.52)	27 (32.14)	20 (23.81)
CHH	1339	248 (18.52)	32 (2.39)	443 (33.08)	413 (30.84)	203 (15.16)
	Recovery genes (**)					
mC	1713 (56.07)	345 (20.14)	43 (2.51)	545 (31.82)	537 (31.35)	243 (14.19)
CG	32 (47.06)	2 (6.25)	0 (0.00)	11 (34.38)	9 (28.13)	10 (31.25)
CHG	46 (54.76)	4 (8.70)	1 (2.17)	13 (28.26)	16 (34.78)	12 (26.09)
CHH	863 (64.45)	175 (20.28)	21 (2.43)	286 (33.14)	252 (29.20)	129 (14.95)

bioRxiv preprint doi: https://doi.org/10.1101/059477; this version posted June 17, 2016. The copyright holder for this preprint (which was not certified by peer review) is the author/funder, who has granted bioRxiv a license to display the preprint in perpetuity. It is made available under aCC-BY-NC-ND 4.0 International license.

Supplementary Tables

Supplementary Table 2: Genome mapping statistics from 9 bisulfite converted Botrytis samples. All samples were mapped to *B. ciniera* B05.10 genome using Bismark/Bowtie2

			Total methylated C's			Total non-methylated C's			% methylation			%mC
Samples	Total bp	% Map. Effic	CpG	CHG	CHH	CpG	CHG	CHH	CpG	CHG	CHH	
T1BS1	26382612	67.6	477254	438983	2499975	130600424	111869938	391807290	0.36	0.39	0.63	0.54
T1BS2	34048060	62.9	526341	485477	2494454	155155501	134341879	485255169	0.34	0.36	0.51	0.45
T1BS3	17347608	61.1	306505	279816	1575956	77226256	66054702	232502707	0.40	0.42	0.67	0.57
AvT1	25926093.33	63.87	436700.00	401425.33	2190128.33	120994060.33	104088839.67	369855055.33	0.36	0.38	0.59	0.52
T8BS1	18543427	62	394348	360641	1568745	83351098	71894819	257263175	0.47	0.50	0.61	0.56
T8BS2	12613134	60.7	248968	229853	902624	55786373	47759672	166229028	0.44	0.48	0.54	0.51
T8BS3	17117307	65.1	391446	360065	2142019	79537475	69135859	257486354	0.49	0.52	0.83	0.71
AvT8	16091289.33	62.60	344920.67	316853.00	1537796.00	72891648.67	62930116.67	226992852.33	0.47	0.50	0.67	0.59
T8PBS1	28336888	62.3	524875	487874	3561078	126943754	110309124	404488048	0.41	0.44	0.87	0.71
T8PBS2	18471780	66.9	435528	403984	2932991	89352607	77332840	279892313	0.49	0.52	1.04	0.84
T8PBS3	14694194	54.3	220458	201667	924438	57483914	49293008	173794940	0.38	0.41	0.53	0.48
AvT8P	20500954.00	61.17	393620.33	364508.33	2472835.67	91260091.67	78978324.00	286058433.67	0.43	0.46	0.86	0.68

bioRxiv preprint doi: https://doi.org/10.1101/059477; this version posted June 17, 2016. The copyright holder for this preprint (which was not certified by peer review) is the author/funder, who has granted bioRxiv a license to display the preprint in perpetuity. It is made available under aCC-BY-NC-ND 4.0 International license.

Supplementary Table 7: Primer sequences used for MSAP.

Oligo name	Function	Sequence
Ad *Hpa*II/*Msp*I	Reverse Adaptor	GACGATGAGTCTAGAA
Ad. *Hpa*II/*Msp*I	Forward Adaptor	CGTTCT AGACTCATC
Ad. *EcoR*I	Reverse Adaptor	AATTGGTACGCAGTCTAC
Ad *EcoR*I	Forward Adaptor	CTCGTAGACTGCGTACC
Pre. *EcoR*I	Preselective primer	GACTGCGTACCAATTCA
Pre. *Hpa*II/*Msp*I	Preselective primer	GATGAGTCCTGAGCGGC
*EcoR*I2	Selective primer	GACTGCGTACCAATTCAAC
*Hpa*II 2.1	Selective primer	GATGAGTCCTGAGCGGCA

bioRxiv preprint doi: https://doi.org/10.1101/059477; this version posted June 17, 2016. The copyright holder for this preprint (which was not certified by peer review) is the author/funder, who has granted bioRxiv a license to display the preprint in perpetuity. It is made available under aCC-BY-NC-ND 4.0 International license.

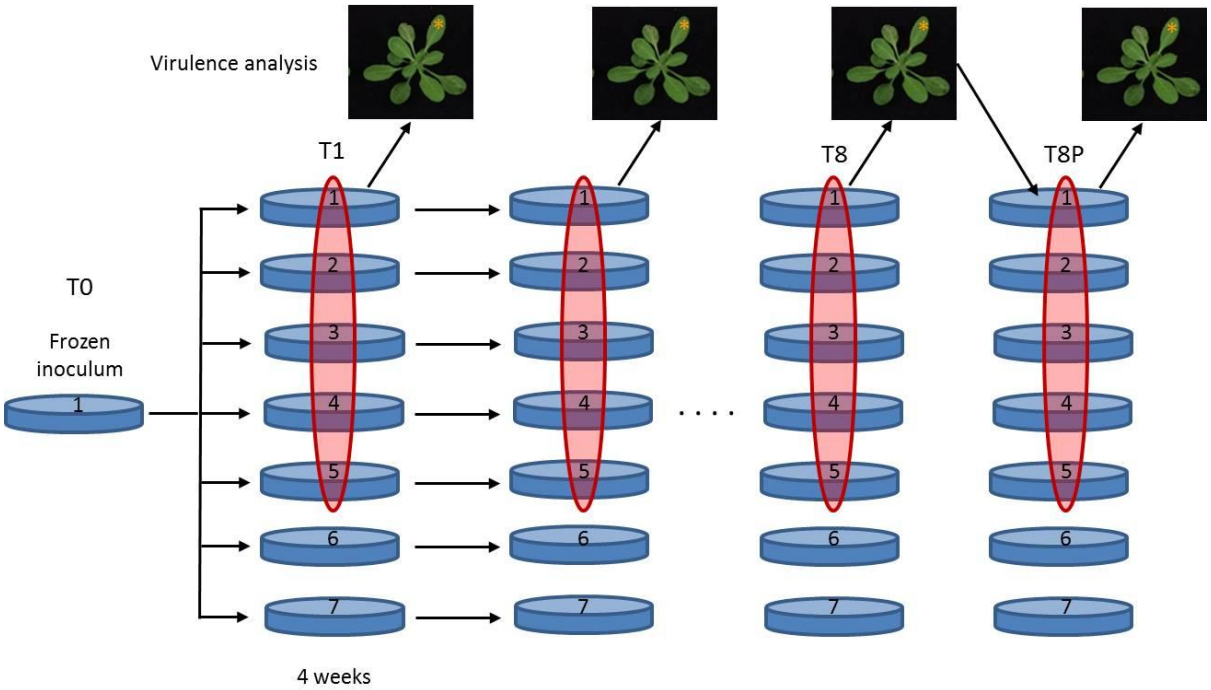

Figure S1: Schematic representation of experimental design. Seven replicated *Botrytis cinerea* cultures were initiated from a single frozen inoculum and cultured for 36 weeks. All replicates were subcultured every 4 weeks to fresh culture medium and mycelia were kept for DNA analysis (MSAPs, WGS, and BS-WGS). Conidia from five randomly selected replicates (highlighted in red) at each time point were collected and used for virulence analysis by inoculating five *Arabidopsis thaliana*. Inoculated *A. thaliana* leaves* at T1, T8 and T8P were collected 72 hours after inoculation for estimation of *in planta* fungal development by quantitative PCR. Conidia from were collected from *A. thaliana* tissue infected with T8 fungus and were re-cultured for a short time to generate conidia to test virulence recovery.

bioRxiv preprint doi: https://doi.org/10.1101/059477; this version posted June 17, 2016. The copyright holder for this preprint (which was not certified by peer review) is the author/funder, who has granted bioRxiv a license to display the preprint in perpetuity. It is made available under aCC-BY-NC-ND 4.0 International license.